

A review on analytical models of brushless permanent magnet machines

A. Abbas¹, A. Iqbal², Arkadiusz Lewicki¹, A. Hosseinpour³

¹ Faculty of Electrical and Control Engineering, Gdansk University of Technology, 80-233 Gdansk, Poland

² Department of Electrical Engineering, Qatar University, Doha, Qatar

³ Department of Electrical Engineering, University of Zabol, Iran

ABSTRACT The electrical machines will be analyzed with the analytical methods as well as numerical methods. However, the numerical models (such as the finite-element method (FEM)) can analyze and model the complex geometries of electrical machines that maybe include saturation effects, but these models have high computational burdens and too time-consuming which is so important in the design stage and optimization issues with too many iterations in electrical machine companies or their related R&D department. Also, the FEM models are not flexible in terms of changing the machine geometries or changing in the input values causing reconstruct the machines for new simulations. Furthermore, the users have no sense of the machine behaviors by applying the numerical models. The abovementioned challenge of the numerical methods can be overcome by analytical models. In principle, analytical methods are introduced based on the magnetic equivalent circuit (MEC) or solving Maxwell's equation. Generally, MEC models are realized as zero-dimensional (0-D) analytical models which are generic and applicable for analyzing various types of electrical machine's topologies that maybe include the saturation effects. Although the MEC models are faster than the numerical model, they are not as accurate as the numerical models for various structures of electrical machines including a great magnetic airgap. Also, the analytical models based on the Maxwell equations are faster than the numerical ones and they have the potential to obtain acceptable accuracy similar to the numerical models in electrical machines. Among all type of electrical machines, the increasing interest of the Brushless permanent-magnet (PM) machines in all low and medium power applications has led to the development of related analytical models. Therefore, this paper interprets the review of the analytical models in these PM machines to explain their recent developments in terms of the machines' quantities such as magnetic flux density components, induced voltage, inductances, electromagnetic force/torque, efficiency or unbalanced magnetic force (UMF). Also, this literature review helps the researchers to save time for determining appropriate references regarding the analytical models of the brushless PM machines. This paper mainly gives the pros and cons of the different analytical models for various PM machines, where the (0-D), (1-D), (2-D) and (3-D) analytical methods has discussed. The Maxwell and basic mathematical analysis for different PM machines has been discussed.

Index Terms *Analytical models, magnetization patterns, Maxwell equations, Numerical models.*

1- INTRODUCTION

The PM machines have been increasingly used in many industrial applications, such as railway traction, servo systems and electric vehicles. Compared to conventional electric machines, PMs provide various advantages like excellent performance, high speed, ultra-lightweight, high efficiency/ reliability, and lower manufacturing cost [1]-[8].

In the designing and optimization process of the PM machines with different geometrical as well as performance characteristic considerations is a challenging task. To reduce time consuming for machine design, research has been carried out to find quick and accurate modeling approach to compute and realize the behavior and performance of PM machines. Analytical models (AM) and Numerical models (NM) are used for analyzing and predicting the machine quantities. The analytical method is essential to minimize the time required for calculation, particularly during the design optimization process. NM become very powerful tools in calculating and predicting machine quantity. However, NMs such as finite element analysis (FEA) are still slow and time

consuming for analyzing the characteristics of the machines [9].

Among various computational techniques to design machines, AM, if possible, plays a significant role since diverse crucial characteristics of motors can be obtained accurately and quickly based on these analytical representations. AM provide electric machine developers with a powerful tool for analysis and investigation of the machine behavior under different operational conditions [10], [11]. AM can be used in electromagnetic torque-calculation, back-EMF waveform prediction, cogging torque calculation and stator iron loss estimation.

AM has many advantages over NM, it significantly requires less computational time which is essential in the optimization goals with many iteration numbers. Also, the user can realize the machine behavior according to the related analytical expression [12]-[17] therefore, AM if possible preferred rather than NM.

Mainly, there are four AM techniques used in machine design: (1) relative permeance model [18], [19]; (2) complex permeance model [20]-[22]; (3) Schwarz-Christoffel mapping [47], [58]. Finally, (4) subdomain (SD) technique [23]-[29]. Zhu *et al.* [30] briefly explained the disadvantages and advantages of all these techniques.

TABLE I
BRUSHLESS PM MACHINES CLASSIFICATION IN TERMS OF
MAGNETIZATION PATTERNS FOR SM OR SI

Magnetization Patterns	Illustrative Representation	Radial Component waveform	Tangential Component Waveform
Radial sinusoidal amplitude magnetization			
Ideal Halbach or sinusoidal angle magnetization			
Radial magnetization			
Parallel magnetization			
Bar magnets in shifting directions or multi-segment Halbach			
Two-segment Halbach			

p is number of pole-pairs
 α_p is magnet-arc per pole-pitch ratio
 k_R and k_T are contribution factor of radial and tangential component respectively

SD technique showed an interesting and high accuracy compared to all other techniques, where the air gap is divided into different subdomains. In this technique, the magnetic flux density in each subdomain is calculated by solving Poisson's equation and applying boundary conditions. However, the calculation of magnetic flux in the stator slot subdomain is redundant and increases the computational volume, a comparison and comprehensive analysis of these models using finite element model as a reference for comparison presented in [31]. The analytical model of brushless permanent magnetic has been reported with different magnetization patterns, such as: radial magnetization; parallel magnetization; sinusoidal amplitude magnetization; ideal Halbach; and multi segment Halbach. Halbach array is a kind of magnetization pattern that magnetic field in one part is stronger than others, also magnetic field in the other point is zero. Information of the six types of magnetization patterns with the radial and tangential components have been represented in Table I, the table represent the radial and tangential components of all different types in surface magnet or inset magnet topologies.

In this paper, the review of the analytical models of the brushless PM machines provides a suitable reference for developing the related future studies that lead to saving time for researching about these models in electrical machines. The machines' quantities such as magnetic flux density components, induced voltage, inductances, electromagnetic force/torque, efficiency or unbalanced magnetic force (UMF) have been considered. Moreover, this paper provides appropriate references regarding the analytical models of the brushless PM machines to help the researchers to obtain more accurate and proper results for their future studies.

2- ANALYTICAL MODELS:

In general, if possible, AM can be divided into four analytical models that is, (0-D), (1-D), (2-D), and (3-D) analytical models.

A. (0-D) Analytical Model:

The (0-D) or Magnetic equivalent circuits (MEC) are used to find the maximum or average value of the magnetic flux, this model can be developed when the rotor has no displacement and the linear part of the magnetization curve is considered to predict the magnetic flux density, it is a suitable candidate when the saturation effects are appeared in some parts of electrical machines [32]. MEC is used to develop the (0-D) analytical model for PM machine. Fig. 1 illustrate the (0-D) formed MEC for slotless linear PMSM.

Where R_m , R_{PM} , R_a , R_s , φ_r are respectively the reluctances of the mover, PM, airgap, stator, and the remanence magnetic flux for the PMs. The maximum magnetic flux density due to PM in the airgap can be computed as,

$$B_g = \frac{\varphi_g}{A_g} \dots \dots \dots (1)$$

The induced voltage can be calculated using MEC as,

$$e_a = -pN_t \omega \frac{2N_t \varphi_g}{\tau_p} y \dots \dots \dots (2)$$

Also, electromagnetic force component can be predicted,

$$F_y = \frac{B_g^2}{4\mu_0} A_g \dots \dots \dots (3)$$

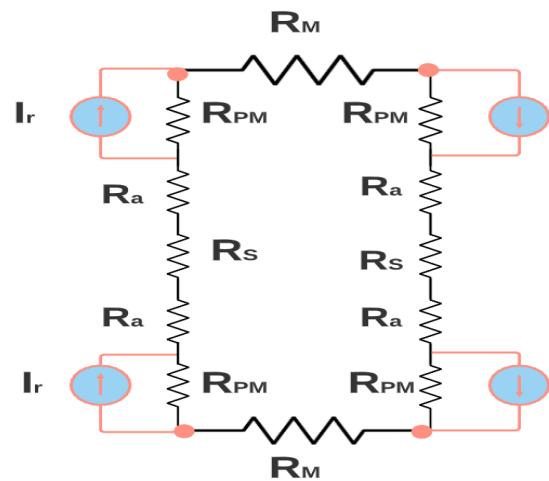


Fig. 1. MEC of slotless linear PM machine

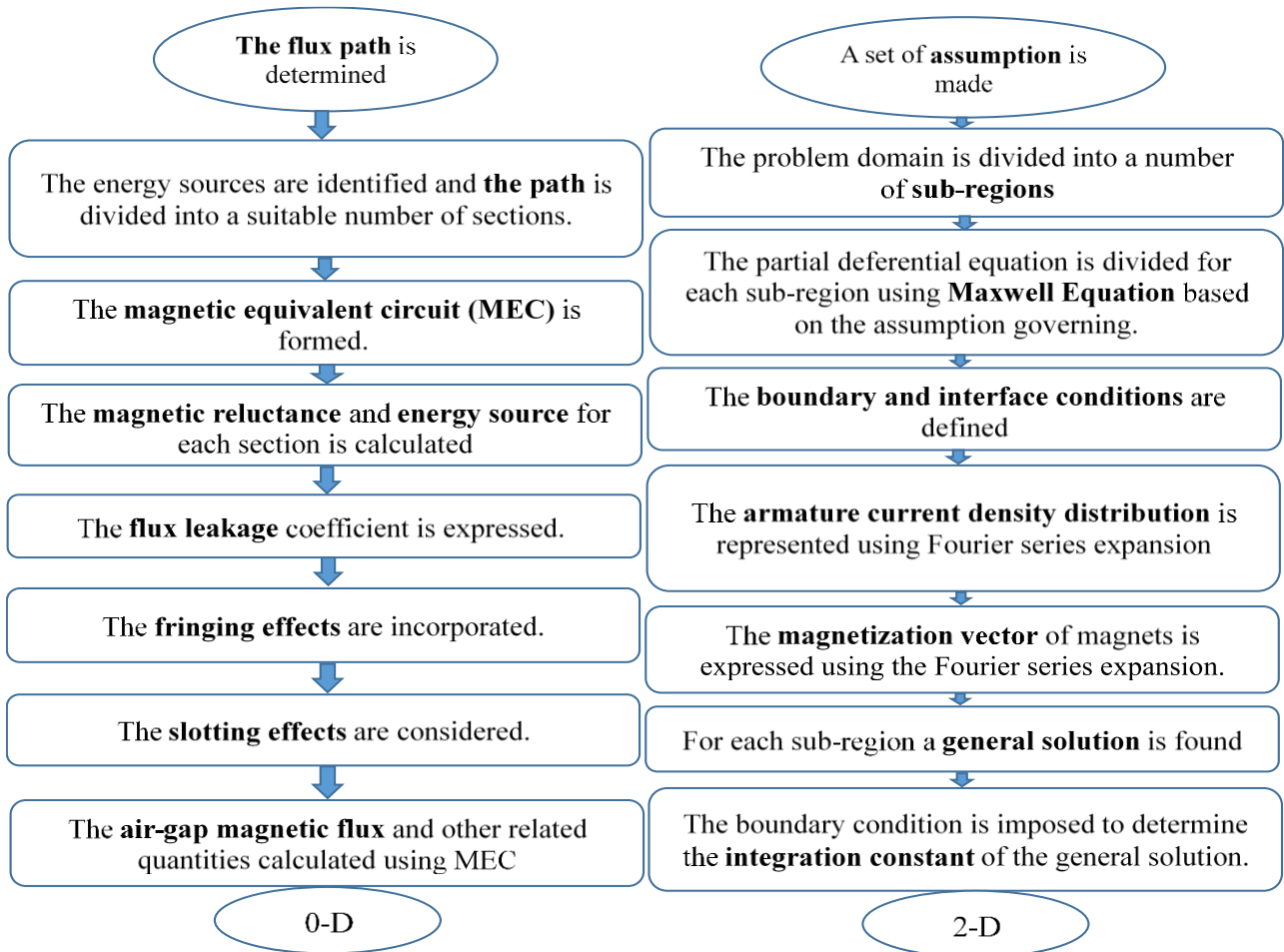


Fig. 2. The procedure of the analytical models.

Based on the equivalent circuit and neglecting the core reluctances the self-inductance is computed as,

$$L_{aa} = \frac{N_c N_f^2}{R_a + R_{PM}} \dots \dots \dots (4)$$

B. (1-D) Analytical Model:

The (1-D) analytical model is suitable when the magnetic flux contains only one component (i.e., radial, or tangential components), such as when the air-gap length is so small that the tangential component of the flux in the airgap can be ignored. But when the air-gap length is such that the tangential component of the flux cannot be neglected, the (1-D) analytical model is no longer appropriate, for example in case of Ss machines [5], [6], [8], [13], [33].

C. (2-D) Analytical Model:

(2-D) analytical model is used to estimates the waveform of the components and calculation of the magnetic flux density, electromagnetic torque, back-electromotive force (EMF) [34], [35]. The (2-D) analytical model is not only fast but also gives physical insight to the problem. Fig. 2 represent the steps for analytical computation of magnetic field for (0-D) and (2-D), the first step is to make some assumptions to relatively simplify the solution of the problem and most importantly to make the analytic solution possible. Secondly divide the machine into regions based on the Maxwell equations and by using the magnetic vector potential. Finally, after applying boundary condition all machine quantities can be

computed [36], [37], and [39]-[46], [49]-[67] and [80]-[86].

Consider a 3-phase Ss brushless machine, the flux linked to the winding of phase k due to magnetic flux produced by the winding of phase j can be expressed as:

$$\phi_{j,k}(t) = p N_t L_s R_x \int_{-\frac{\theta_c}{2p} + 2\pi(k-1)/pq}^{\frac{\theta_c}{2p} + 2\pi(k-1)/pq} B_{r,j}^x(R_x, \theta, t) d\theta \dots \dots \dots (5)$$

For $k= 1, 2, 3$ and $j=1, 2, 3$ where $B_{r,j}^x$ is the radial component of the flux density, θ_c is the coil pitch angle and R_x is the radius at the middle of the winding region. the magnetic flux density in the airgap, the electromagnetic torque can be computed as,

$$T(t) = \frac{L_s R_c^2}{\mu} \int_{-\pi}^{\pi} \frac{1}{\mu} (B_{R,PM}^a B_{T,PM}^a + B_{R,PM}^a B_{T,PM}^a + B_{R,PM}^a B_{T,AR}^a + B_{T,AR}^a B_{T,AR}^a) \dots \dots \dots (6)$$

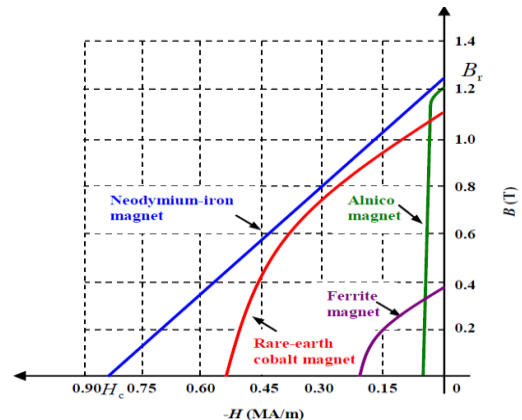
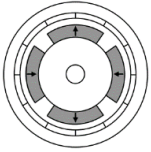
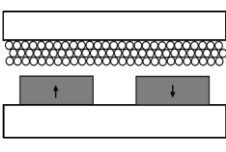
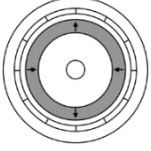
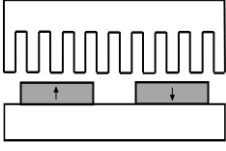
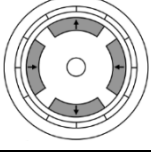
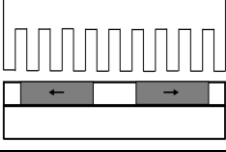
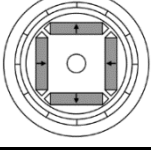
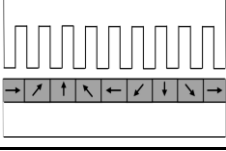
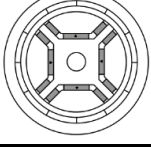
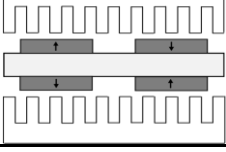
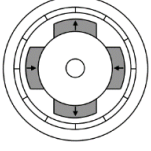
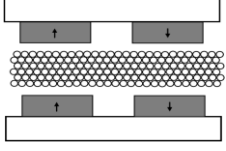
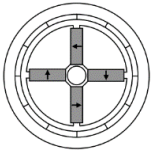
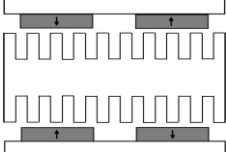
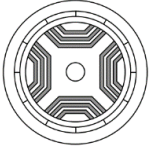
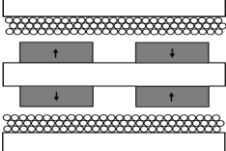


Fig. 3. Demagnetization curve of four types of permanent magnets

TABLE II: BRUSHLESS PM MACHINES CLASSIFICATION IN TERMS OF MAGNET AND MACHINE STRUCTURES

ROTARY STRUCTURES		LINEAR STRUCTURES	
Surface-mounted magnet		Slotless and surface-mounted parallel magnet	
Ring magnet		Slotted and surface-mounted parallel magnet	
Surface-inset magnet		Slotted and buried or interior magnet	
Buried or interior magnet		Slotted with Halbach array magnet	
Multi-segment interior magnet		Double sided and slotted outer armature	
Surface-mounted magnet with parallel edges		Double sided and slotless with one inner armature	
Spoke Magnet		Double sided and slotted inner armature	
Multilayer Interior Magnet		Double sided and slotless outer armature	

D. (3-D) Analytical Model:

The (3-D) analytical models are not used widely because of the difficulty and complexity of the deriving (3-D) analytical equations, a (3-D) AM is highly time consuming specially in designing structure of PM machines. Sometimes, it is necessary to apply assumptions to simplify the obtained model. It may also be necessary to combine the analytical and numerical (3-D) models [38], [47], [68], [75], [78], [92], and [100].

From the literature review (2-D) analytical model is a potential candidate to analyze and predict various machine quantities, in the terms of the accuracy of the magnetic flux density, induced voltage, self and mutual inductances as well as the tangential and normal electromagnetic forces. Researchers prefer to use this approach due to its speed and shorter computational time compared to other SD techniques.

PMs can be classified according to PM topology as; surface inset (*SI*) [39]-[43], surface mounted (*SM*) [44]-[48], spoke PM (*SPM*) and buried or interior PM (*BPM*) [49]-[51]. Fig. 3 demonstrates comparison of four types of permanent magnet. The cost of manufacturing interior magnet is very high [52], compared to surface-mounted, surface-inset provide a compromise with several advantages such as: lower PM eddy current losses, higher rotor mechanical robustness, higher quadrant-per direct-axis reactance, better filed weakening region [53], [54]. Table II above illustrate different types of magnet structure for linear and rotary machines.

The stator structure of PM machine can be classified as *Sd* and *Ss* structures *Sd* stator structure has more air-gap flux density due to less magnetic airgap and includes better heat removal compared with the *Ss* structure. On the other hand, the *Ss* stator structure reduces the cogging torque and cost of winding. Also, the suitable space for winding exists in the *Ss* structures. Common types of The PM machines include NdFeB, Sm2Co17, SmCo5, Alnico-5 and Ferrite, in which three processes of providing these materials are sintering, injection molding, compression bonding and casting. Table III compare between *Sd* and *Ss* structure of stator.

TABLE III: A COMPARISON BETWEEN SLOTTED AND SLOTLESS STATOR STRUCTURE

	Slotted (<i>Sd</i>)	Slotless (<i>Ss</i>)
Cogging torque	Exist	Almost nothing
Cost of winding	Higher	Lower
Magnetic airgap	Smaller	Lower
Air-gap flux density	Higher	Lower
Inductance	Higher	Lower
Heat removal	Better	Worse
Winding space	Lower	Higher

2- PROCEEDINGS AND ANALYTICAL PROCEDURES

Electromagnetic devices can be modeled and analyzed either analytically or numerically. However generally, numerical approaches, (i.e., finite element method (FEM)), are widely employed to analyze the performance and present an accurate modeling of electrical machines, but this method has some limitations and takes a long computation time to achieve the result. Therefore, the requirement to reduce pre-design stages duration and time-consuming process by analytical solutions, if possible, are preferred frequently. Several types of analytical methods such as magnetic equivalent circuits (MEC), conformal mapping (i.e., Schwarz-Christoffel) and sub-domain method are often used so that any of them have different techniques. Based on the mentioned methods, the sub-domain [55] technique due to the high speed and precision is more famous. In this way, analytical models are divided to regions according to the shape and material characteristics, (i.e., magnet, air gap, and winding) and according to partial differential equations (PDEs) that are derived from Maxwell's equations, due to a set of assumptions, the problem is simplified and a general solution, which provides the PDEs and boundary

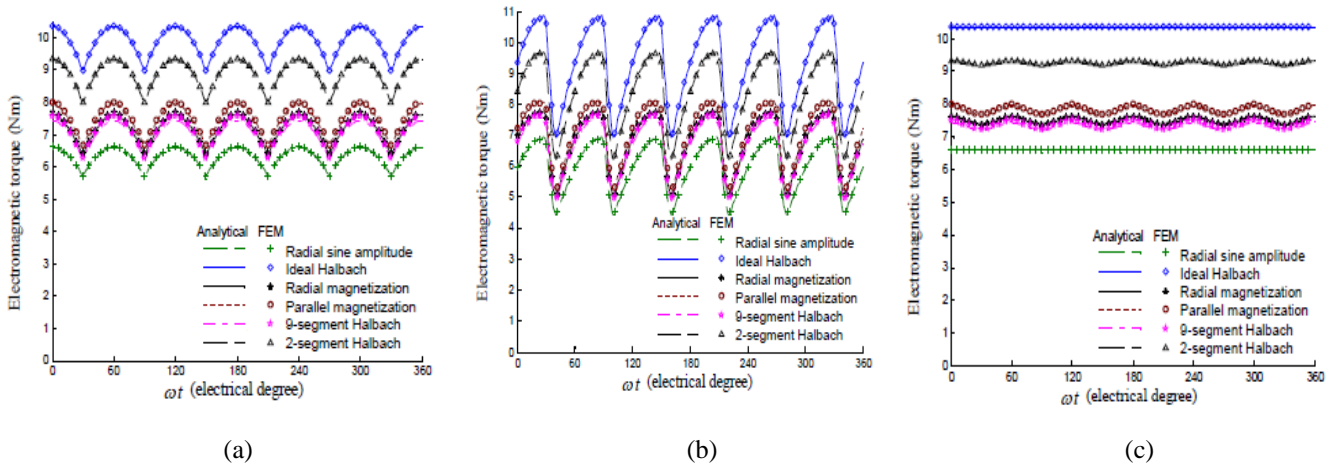


Fig. 5 Electromagnetic torque in the case of the internal rotor motor; a) With the ideal rectangular current waveform; b) With the six-step rectangular current waveform; c) With the sinusoidal current waveform.

conditions for each region. Fig. 4 illustrate the sub-domains of PM machines with Q slots and p pole-pairs.

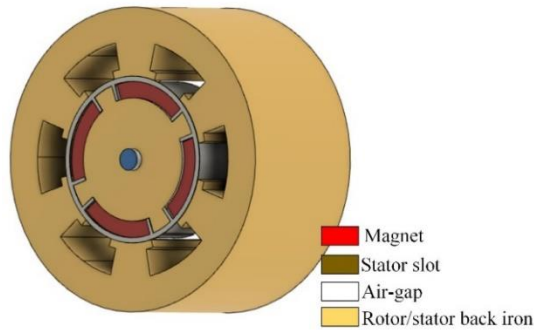


Fig. 4 Illustrative representation of PMSM sub-domains

A. List of Assumptions:

The important assumption in the subdomain technique is related to iron parts, the following assumptions are made to either enable or simplify the analytical model:

- End effects are ignored, that is, the motor is assumed to have infinite axial length.
- The magnetic flux density vector has only radial and tangential components
- The media have finite permeability and linear magnetization characteristic. The saturation effects of the media are neglected.
- The airspace between the magnets has the same permeability as the magnets.
- Eddy current reaction field is neglected.

It is noted that importance of accurate determination of the magnetic field distribution (as for PM and armature reaction) in the air gap of permanent magnet machines is identified to evaluate the machine performance meanwhile, the air gap magnetic field computation can be assessed by numerical (i.e., FEM) or analytical methods. In the most analytical papers, machine quantities such as magnetic field distributions, a back electromotive force (Back-EMF) and electromagnetic torque (cogging torque and load torque) are computed with the proposed analytical method and verified by finite element analysis. Fig. 5 (a-c) illustrate the ideal rectangular, six-step rectangular and sinusoidal current waveforms, for electromagnetic torque [56].

B. Governing PDEs:

Based on Maxwell's equations, partial differential equations (PDEs) can be represented, and the armature current density distribution can also be expressed using its Fourier series expansion. A set of assumptions for the designed machine must be made to simplify the calculations.

A methodology for study the problem resolution for magnetism is presented by Ampere's law $\nabla \cdot \mathbf{B} = 0$ and Gauss's law $\nabla \times \mathbf{H} = \mathbf{J}$, wherein \mathbf{H} is the magnetic field intensity vector and \mathbf{J} is the electric current density vector. The corresponding relationship between magnetic field density vector and magnetic field intensity vector is expressed as follow:

$$\mathbf{B} = \mu_0 \mu_r \mathbf{H} + \mu_0 \mathbf{M} \dots\dots\dots (7)$$

Where μ_0 is the free space permeability, μ_r is the relative permeability and \mathbf{M} is the magnetization vector in A/m. with substituting equation (1) in Ampere's circuital law, yields:

$$\nabla \times \mathbf{B} = \mu_0 \mu_r \nabla \times \mathbf{H} + \mu_0 \nabla \times \mathbf{M} \dots\dots\dots (8)$$

According to gauss's law, magnetic flux is determined as follow:

$$\mathbf{B} = \nabla \times \mathbf{A} \dots\dots\dots (9)$$

With substituting (3) into (2) and considering $\nabla \cdot \mathbf{A} = 0$, governing equation is achieved as follow:

$$\nabla^2 \mathbf{A} = -\mu_0 \mu_r \mathbf{J} - \mu_0 \nabla \times \mathbf{M} \dots\dots\dots (10)$$

By the use of separated variables technique, the general solution of the Laplace and Poisson equation for each region can be obtained.

$$\nabla^2 \mathbf{A}^w = -\mu_0 \mathbf{J} \dots\dots\dots (11)$$

$$\nabla^2 \mathbf{A}^m = -\mu_0 \nabla \times \mathbf{M} \dots\dots\dots (12)$$

$$\nabla^2 \mathbf{A}^i = 0 \dots\dots\dots (13)$$

Where superscripts $\{w, m\}$ designate the winding and magnet, respectively and $\{i\}$ is representative of other regions such as exterior, stator, airgap, retaining sleeve, rotor and shaft regions that are indicated by $\{a, sl, \text{ and } so\}$ respectively. Fig. 6 [57] demonstrate the value of radial

and tangential open circuit flux density for internal rotor in the winding region and Fig. 7 [53] show flux density due to armature field in the middle of air gap for different electrical degrees.

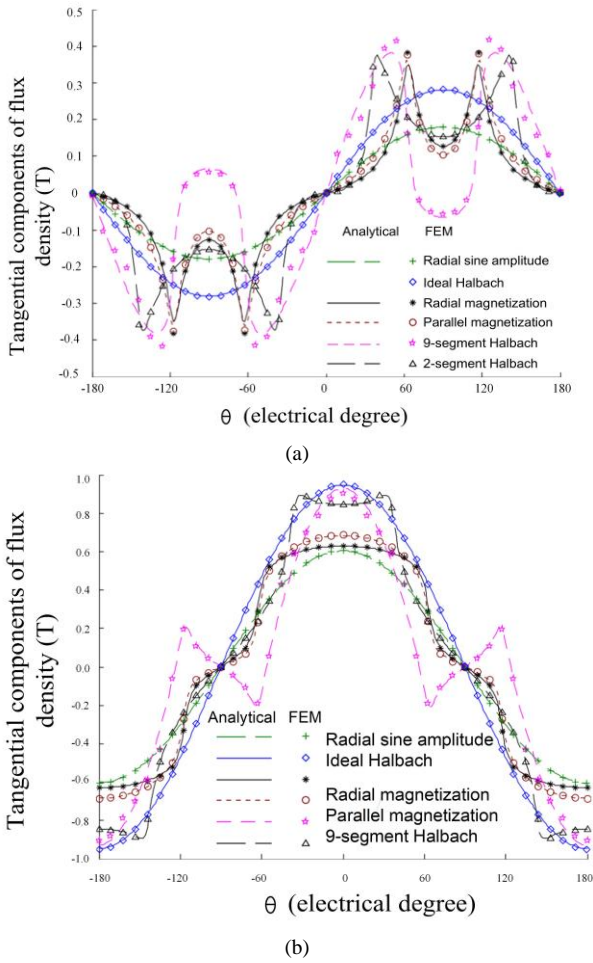


Fig. 6 (a) Flux density of the internal rotor in tangential component, (b) Flux density of the internal rotor in radial component

C. Boundary Conditions:

According to the extracted PDEs, the boundary conditions play substantial roles in solving these equations and obtaining the value of each variable in the magnetic flux density components. The boundary conditions can be categorized into two main groups as follows [58]-[60]:

1. the normal component of the magnetic flux density vector is continuous at the interfaces between two adjacent media ($\mathbf{B}_{\perp}^i = \mathbf{B}_{\perp}^{i+}$) where i and $i+$ are two adjacent sub-region).

2. In the case of the source-free interface, the tangential component of the magnetic field intensity vector is continuous at that interface ($\mathbf{H}_{\parallel}^i = \mathbf{H}_{\parallel}^{i+}$).

After imposing the boundary interface conditions given in Table IV of Appendix A (internal/external rotor machine), a set of simultaneous algebraic equations with the number of defined unknown variables can be formed to solve PDEs.

E. Extracting the Magnetic Model:

The machine divided into several sub-regions, and partial differential equation extracted for each part based on Maxwell’s equations. In this section mathematical equations for slotted/slotless or inner/outer rotor machine represented, these equations can be used to design any PMSM machine of any number of phases, slots, and poles.

Also, the equations mentioned in this paper is suitable for internal or external rotor machines.

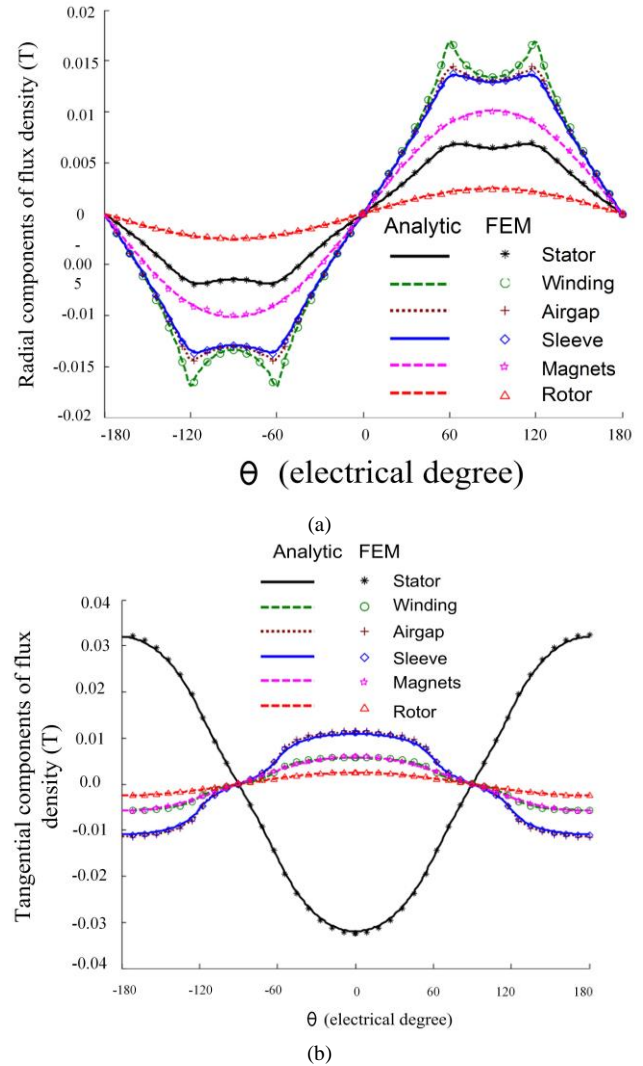


Fig. 7 (a) Flux density in the middle of air gap due to AR field in radial component, (b) Flux density in the middle of air gap due to the AR in tangential component.

1. Extracting FS of AR Currents:

The current of each phase of PMSM can be represented as $i_j(t) = \sum_u I_m \sin [u(pwt - \gamma_j) + \theta_m]$ (13)

The current density distribution of a 3-phase winding

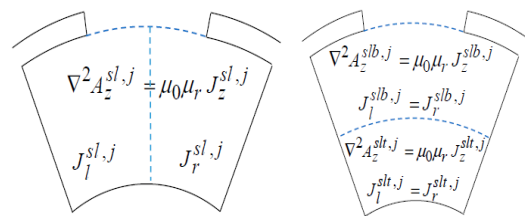


Fig. 8 Winding configuration

depends on winding configuration, there are two common types of configurations, overlapping and nonoverlapping winding, the distribution of current density represented in Fig. 8. Using equation (11), current density is determined by its Fourier series as follows:

$$J(\theta, t) = J_0^j(t) + \sum_{v=1}^V J_v^j(t) \cos (\frac{\pi v}{\delta} (\theta - \theta_j + \delta/2)) \dots (14)$$

$\theta_j = 2\pi(j - 0.5)/Q$ The angle of the center of slot j w.r.t. x-axis.

where $j_0^j(t)$ and $j_v^j(t)$ are as follows:

$$j_0^j(t) = \frac{j_\ell^j(t) + j_r^j(t)}{2} \quad \& \quad j_v^j(t) = \frac{j_\ell^j(t) - j_r^j(t)}{\pi v/2} \sin(\pi v/2)$$

2. Extracting FS of PM Magnetization Pattern:

In (2-D) AM considering polar coordinates coordinate, the magnetization vector can be expressed as,

$$M = M_R r + M_T \theta$$

The radial and tangential components for radius independent magnetization are expressed as,

$$M_{Rx}^k(\theta) = \sum_{x=1,3,5,\dots}^X M_{Rx}^k \sin\left(\frac{xp}{\alpha_r} \left(\theta - \alpha - \frac{2k\pi}{p} + \frac{\alpha_r \pi}{2p}\right)\right) \dots (15)$$

$$M_{Tx}^k(\theta) = \sum_{x=1,3,5,\dots}^X M_{Tx}^k \cos\left(\frac{xp}{\alpha_r} \left(\theta - \alpha - \frac{2k\pi}{p} + \frac{\alpha_r \pi}{2p}\right)\right) \dots (16)$$

Depending on different magnetisation patterns illustrative in Table I, M_{Rx}^k & M_{Tx}^k can be defined as follows:

In the case of *radial* magnetization:

$$\left. \begin{aligned} M_{Rx}^k &= \frac{4 B_{rem}}{\mu_o x \pi} \sin\left(\frac{x \pi \alpha_p}{2 \alpha_r}\right) \\ M_{Tx}^k &= 0 \end{aligned} \right\} \dots (17)$$

In the case of *Parallel* magnetization:

$$\left. \begin{aligned} M_{Rx}^k &= \frac{4 B_{rem} \alpha_p}{\mu_o \alpha_r} [A_{1x}(\alpha_p, \alpha_r) + A_{2x}(\alpha_p, \alpha_r)] \\ M_{Tx}^k &= \frac{4 B_{rem} \alpha_p}{\mu_o \alpha_r} [A_{1x}(\alpha_p, \alpha_r) - A_{2x}(\alpha_p, \alpha_r)] \end{aligned} \right\} \dots (18)$$

Where

$$A_{1x}(\alpha_p, \alpha_r) = \frac{\sin((xp + \alpha_p) \frac{\pi \alpha_p}{2p \alpha_r})}{(xp + \alpha_p) \frac{\pi \alpha_p}{2p \alpha_r}}$$

$$A_{2x}(\alpha_p, \alpha_r) = \begin{cases} \frac{\sin((xp + \alpha_p) \frac{\pi \alpha_p}{2p \alpha_r})}{(xp + \alpha_p) \frac{\pi \alpha_p}{2p \alpha_r}}, & xp \neq \alpha_r \\ 1, & xp = \alpha_r \end{cases}$$

In the case of *Halbach* magnetization:

$$M_{Rx}^k = -\frac{4 B_{rem} \alpha_p}{\mu_o \alpha_r} \frac{\cos\left(\frac{\pi \alpha_p}{2 \alpha_r}\right)}{\left(\frac{x \alpha_p}{\alpha_r}\right)^2 - 1}, \quad x \alpha_p \neq \alpha_r \dots (19)$$

$$M_{Tx}^k = \frac{B_{rem} \alpha_p}{x \mu_o}, \quad x \alpha_p = \alpha_r \dots (20)$$

The expected waveform of radial and tangential components of all different types of magnetization pattern presented in Table I.

3. Extracting equations to calculate flux density:

Based on infinite permeability assumption of the machine stator and rotor back iron, four different regions are defined to extract flux density due to both AR and PM: 1) magnet; 2) airgap; 3) slot 4) slot-opening.

The flux density calculation for all sub-regions due to AR and PM for internal/external rotor machine can be represented in Table V of Appendix A

By applying the interfacing conditions (section C) and using the correlation technique [107], [157], the integral constants are obtained for both internal/ external rotor machine in Appendix B. These equations can be used to design slotted/ slotless machine with any combination of pole-pairs.

3-MACHINE QUANTITIES:

Accurate magnetic field calculations of brushless PM machines are essential to compute other electromagnetic quantities. Mainly there are two sources of the magnetic field distribution: the permanent magnets (PMs) and the armature winding current. Based on the superposition principle, the solution of the electromagnetic problem is equal with a linear combination of the open-circuit magnetic field problem ($J = 0$) [62], and the armature reaction magnetic field problem ($M = 0$) [67].

Based on the open circuit flux density, flux linked with each coil, induced back-emf in the armature winding, stator eddy current losses, winding eddy current losses, local traction and cogging torque can be obtained [101], [107].

A. Flux Linkage and Induced Voltage:

The first phase winding flux linkages are estimated from the calculated flux density of the subregions in the same winding and the presence of due to the PMs is given below,

$$\lambda_a = N_t N_c \int B^w \cdot dS \dots (21)$$

Where λ_a is the phase- a flux linkages and B^w is the flux density component because of PM in the middle of winding linked with the phase “ a ”. With the help of Faraday’s law, the induced voltage of phase “ a ” can be deduced using the following equation,

$$E_a = \frac{d\lambda_a}{dt} \dots (22)$$

B. Inductance:

The inductances of the analytical machine model are not depending on the armature current where the saturation effects are neglected. The self and mutual inductance are calculated as the following expression:

$$L_{aa} = \frac{\lambda_{aa}}{i_a} \dots (23)$$

$$L_{ab} = \frac{\lambda_{ab}}{i_a} \dots (24)$$

Here L_{aa} is phase- a self-inductance, L_{ab} is the mutual inductance of phase- a and phase- b , λ_{ab} flux linkages of phase- b due to the phase- a and i_a phase- a current.

C. Torque:

By employing both flux densities (i.e., produced by armature reaction and PMs), the electromagnetic torque and unbalanced magnetic forces are computed. The instantaneous developed torque consists of cogging, electromagnetic and reluctance components.

$$T(t) = T_{cog}(t) + T_{em}(t) + T_{rel}(t) \dots (25)$$

$$T(t) = L_s \int_{-\pi}^{\pi} \frac{1}{\mu_o} (B_{R,PM}^a + B_{R,AR}^a) (B_{T,PM}^a + B_{T,AR}^a) \Big|_{r=R_c} R_c^2 d\theta \dots (26)$$

Where $R_c = \frac{R_a + R_{sl}}{2}$

D. Unbalance Magnetic Force (UMF):

Another important quantity in PM machines is unbalance magnetic force, based on Maxwell stress tensor the radial and tangential components of the magnetic local traction acting on each rotor surface can be obtained as

$$F_x(t) = L_s \int_{-\pi}^{\pi} (f_r \cos\theta - f_\theta \sin\theta) r d\theta \dots\dots\dots (27)$$

$$F_y(t) = L_s \int_{-\pi}^{\pi} (f_r \sin\theta + f_\theta \cos\theta) r d\theta \dots\dots\dots (28)$$

Where

$$F_r = \frac{1}{2\mu_0} (B_n^2 - B_t^2) \quad \& \quad F_\theta = \frac{1}{\mu_0} (B_r B_\theta)$$

The magnitude of the unbalanced force can be obtained as

$$|F| = \sqrt{(F_x^2(t) + F_y^2(t))} \dots\dots\dots (29)$$

4. Review of Analytical Modeling for Various Permanent Magnet Machines:

Table VI in Appendix C represent summary of the references published on the analytical modeling of brushless permanent magnet synchronous machines (PMSM).

Over the past 30 years, a large contribution has been made on AM to solve and design PMSM. A summarized review of AM techniques used to solve the magnetic field on PMSM presented in Table VI. In this table the calculation of flux density and all other machine quantities for *Sd/Ss*, internal/external rotor machine using different magnetization pattern has been addressed [1-250].

The third and fourth column of Table VI, the direction of motion and flux for all publication is mentioned, the most common configuration used to design brushless PMSM are Axial and Radial configurations, in terms of power density, stator manufacturing cost and number of poles, axial flux configuration is a potential candidate that produces higher flux, but this configuration failed to be used in case of high power PMSMs.

In fifth column, the structure of PMSM stator has been classified, there are mainly two types of stators, *Sd* or *Ss* stator. Slotted machines preferred due to its higher airgap flux density and provide better heat removal, the comparison between *Ss* and *Sd* given in Table III. The calculation of slotting effects has been considered in some papers using either conformal transformation techniques [1], [4], [6], [13], [19]- [22], [66] or subdomain technique (SD) [7], [23]-[30], [39- [42], [52]-[56], [96], [128], [137], [145], [156], [165], [176], [189], [200], [205], [209], [213], [226], [228], [229]. The advantage and disadvantages of conformal transformation technique has been explained briefly by *Zhu et al.* [30].

In brushless PMSM there are two sources to generate the magnetic field, the first one is armature reaction (AR), by predicting armature field distribution PMSM, it's easy to calculate the self and mutual inductances and computing the eddy current loss in all different part of the machine. The second one is PM which can be used to calculate the magnetic flux linked with each coil, the electromotive force (EMF) induced in each phase, cogging torque and unbalance magnetic forces (UMFs). There are some

quantities of PMSM require both AR and PM, like electromagnetic torque.

In sixth column, the location and topology of PM has been presented for PMSM machines as illustrated in Table II (in introduction section), the most used are topologies are *SM*, *SI* and *SPM* and *BPM*. In terms of cost *SM* and *SI* show low cost but for *BPM* the cost is very high but in case of magnetic eddy current losses, *SM* showing high cost compared to other topologies.

There are different types of magnetization pattern considered when designing PMSM, such as: radial; ideal Halbach; parallel; sinusoidal amplitude; and segmented-Halbach, as shown in the seventh column of the table.

Another criterion of the classification is the number of dimensions, the formulation dimensions carried out in polar or rectangular (Cartesian) coordinates, as indicated for each reference in the eighth column of Table VI. Last column of Table V represents the various consideration and calculations of each reference [1] – [75].

5. CONCLUSION

This literature review has investigated the analytical models of the brushless PM machines to provide a suitable reference for developing the related future studies that lead to saving time for researching these models in electrical machines. For the aim, such as flexible in terms of changing the machine geometries or changing the input values, low computational burdens and low time-consuming, the analytical models are recommended to overcome the mentioned challenges.

The review of the analytical models in these PM machines explains their recent developments in terms of the machines' quantities such as magnetic B components, induced voltage, Inductances, electromagnetic F/T, η and UMF. Also, one of the applicable methods for studying different types of the brushless PM machines classification in terms of magnet and machine structures are considered in this review. Comparison of characteristics such as flux direction, stator structure, permanent magnet configuration, magnetization pattern, number of dimensions, coordinate, magnetic potential, PM, and AR reaction effects are performed. By comparing the used methods and obtained results in the articles, the accuracy and speed of the analytical expressions and the efficacy of the analytical approach have been confirmed. This paper summarizes [250] publications to help the researchers to save time for determining appropriate references regarding the analytical models of the brushless PM machines.

TABLE IV The Boundary Conditions of PM machine

Region 1	Region 2	Boundary	Interface	Range
Magnet k	Rotor iron	$H_T^{m,k}(r, \theta) = 0$	$r = R_r$	$\left \theta - \alpha - \frac{2k\pi}{p} \right \leq \frac{\alpha_r\pi}{2p}$
Magnet k	Both sides iron-pole	$H_R^{m,k}(r, \theta) = 0$	$\theta = \alpha - \frac{2k\pi}{p} \pm \frac{\alpha_r\pi}{2p}$	$R_r \leq r \leq R_m$
Airgap	Magnet k	$B_R^a(r, \theta) = B_R^{m,k}(r, \theta)$	$r = R_m$	$\left \theta - \alpha - \frac{2k\pi}{p} \right \leq \frac{\alpha_r\pi}{2p}$
Airgap	Magnets & iron-poles	$H_T^a(r, \theta) = \begin{cases} \sum_{k=0}^{p-1} H_T^{m,k}(r, \theta) \\ 0 \end{cases}$	$r = R_m$	$\begin{cases} \left \theta - \alpha - \frac{2k\pi}{p} \right \leq \frac{\alpha_r\pi}{2p} \\ \text{else where} \end{cases}$
Slot-opening j	Both sides tooth-tip	$H_T^{so,j}(r, \theta) = 0$	$\theta = \theta_j \pm \beta$	$R_s \leq r \leq R_{so}$
Airgap	Slot-opening j	$B_R^a(r, \theta) = B_R^{so,j}(r, \theta)$	$r = R_s$	$\begin{cases} \theta_j - \frac{\delta}{2} \leq \theta < \theta_j - \frac{\beta}{2} \\ \theta_j - \frac{\delta}{2} \leq \theta \leq \theta_j - \frac{\beta}{2} \\ \theta_j - \frac{\delta}{2} < \theta \leq \theta_j - \frac{\beta}{2} \end{cases}$
Airgap	Slot-openings & teeth	$H_T^a(r, \theta) = \begin{cases} \sum_{j=0}^Q H_T^{so,j}(r, \theta) \\ 0 \end{cases}$	$r = R_s$	$ \theta - \theta_j \leq \frac{\beta}{2}$
Slot j	Slot-opening j	$B_R^{sl,j}(r, \theta) = B_R^{so,j}(r, \theta)$	$r = R_{so}$	$\begin{cases} \theta - \theta_j \leq \frac{\beta}{2} \\ \text{else where} \end{cases}$
Slot j	Tooth-tip Slot-opening j Tooth-tip	$H_T^{sl,j}(r, \theta) = \begin{cases} 0 \\ H_T^{so,j}(r, \theta) \\ 0 \end{cases}$	$r = R_{so}$	$ \theta - \theta_j \leq \frac{\beta}{2}$
Slot j	Both sides tooth	$H_R^{sl,j}(r, \theta) = 0$	$\theta = \theta_j \pm \delta_j$	$R_s \leq r \leq R_{so}$
Slot j	Stator back-iron	$H_T^{sl,j}(r, \theta) = 0$	$r = R_{sl}$	$ \theta - \theta_j \leq \frac{\delta}{2}$

TABLE V Radial and Tangential Components of flux density for internal/external rotor slotted machine

Regions	B_R & B_T Components	limits
Magnet k	$B_R^{m,k}(r, \theta) = - \sum_{t=1}^T \bar{t} \left\{ \frac{a_t^{m,k}}{R_m} \left[\left(\frac{r}{R_m} \right)^{\bar{t}-1} + \left(\frac{R_r}{R_m} \right)^{\bar{t}-1} \left(\frac{R_r}{r} \right)^{\bar{t}+1} \right] + \xi_{t1}^k \left(\frac{R_r}{r} \right)^{\bar{t}-1} + k_t^k r \right\} \sin \left(\bar{t} \left(\theta - \alpha - \frac{2k\pi}{p} + \frac{\alpha_r\pi}{2p} \right) \right)$ $B_T^{m,k}(r, \theta) = - \sum_{t=1}^T \bar{t} \left\{ \frac{a_t^{m,k}}{R_m} \left[\left(\frac{r}{R_m} \right)^{\bar{t}-1} - \left(\frac{R_r}{R_m} \right)^{\bar{t}-1} \left(\frac{R_r}{r} \right)^{\bar{t}+1} \right] + \xi_{t1}^k \left(\frac{R_r}{r} \right)^{\bar{t}-1} + k_t^k r \right\} \cos \left(\bar{t} \left(\theta - \alpha - \frac{2k\pi}{p} + \frac{\alpha_r\pi}{2p} \right) \right)$	$R_r \leq r \leq R_m$ $\left \theta - \alpha - \frac{2k\pi}{p} \right \leq \frac{\alpha_r\pi}{2p}$
Airgap	$B_R^a(r, \theta) = - \sum_{x=1}^X x \left\{ \left[\frac{a_x^a}{R_s} \left(\frac{r}{R_m} \right)^{x-1} + \frac{b_x^a}{R_m} \left(\frac{R_m}{r} \right)^{x+1} \right] \sin(x\theta) - \left[\frac{c_x^a}{R_s} \left(\frac{r}{R_m} \right)^{x-1} + \frac{d_x^a}{R_m} \left(\frac{R_m}{r} \right)^{x+1} \right] \cos(x\theta) \right\}$ $B_T^a(r, \theta) = - \sum_{x=1}^X x \left\{ \left[\frac{a_x^a}{R_s} \left(\frac{r}{R_m} \right)^{x-1} - \frac{b_x^a}{R_m} \left(\frac{R_m}{r} \right)^{x+1} \right] \cos(x\theta) - \left[\frac{c_x^a}{R_s} \left(\frac{r}{R_m} \right)^{x-1} - \frac{d_x^a}{R_m} \left(\frac{R_m}{r} \right)^{x+1} \right] \sin(x\theta) \right\}$	$R_m \leq r \leq R_s$
Slot-opening j	$B_R^{so,j}(r, \theta) = - \sum_{y=1}^Y \bar{y} \left\{ \frac{a_y^{so,j}}{R_{so}} \left[\left(\frac{r}{R_{so}} \right)^{\bar{y}-1} + \frac{b_y^{so,j}}{R_s} \left(\frac{R_s}{r} \right)^{\bar{y}+1} \right] \right\} \sin \left(\bar{y} \left(\theta - \theta_j + \frac{\beta}{2} \right) \right)$ $B_T^{so,j}(r, \theta) = - \frac{b_y^{so,j}}{r} - \sum_{y=1}^Y \bar{y} \left\{ \frac{a_y^{so,j}}{R_{so}} \left[\left(\frac{r}{R_{so}} \right)^{\bar{y}-1} - \frac{b_y^{so,j}}{R_s} \left(\frac{R_s}{r} \right)^{\bar{y}+1} \right] \right\} \cos \left(\bar{y} \left(\theta - \theta_j + \frac{\beta}{2} \right) \right)$	$R_s \leq r \leq R_{so}$ $ \theta - \theta_j \leq \frac{\beta}{2}$
Slot j	$B_R^{sl}(r, \theta) = - \sum_{z=1}^Z \bar{z} \left\{ \frac{b_z^{sl,j}}{R_{so}} \left[\left(\frac{R_{so}}{R_{sl}} \right)^{\bar{z}+1} \left(\frac{r}{R_{sl}} \right)^{\bar{z}-1} + \left(\frac{R_{so}}{r} \right)^{\bar{z}+1} \right] + \frac{\mu_{0j}^j}{\bar{z}^2 - 4} \left[r - \frac{2R_{sl}}{\bar{z}} \left(\frac{r}{R_{sl}} \right)^{\bar{z}-1} \right] \right\} \sin \left(\bar{z} \left(\theta - \theta_j + \frac{\delta}{2} \right) \right)$ $B_T^{sl}(r, \theta) = - \frac{\mu_{0j}^j}{2} \left[\frac{R_{sl}}{r} - r \right] - \sum_{z=1}^Z \left\{ \frac{b_z^{sl,j}}{\bar{z}} \left[\left(\frac{R_{so}}{R_{sl}} \right)^{\bar{z}+1} \left(\frac{r}{R_{sl}} \right)^{\bar{z}-1} - \left(\frac{R_{so}}{r} \right)^{\bar{z}+1} \right] + \frac{2\mu_{0j}^j}{\bar{z}^2 - 4} \left[r - R_{sl} \left(\frac{r}{R_{sl}} \right)^{\bar{z}-1} \right] \right\} \cos \left(\bar{z} \left(\theta - \theta_j + \frac{\delta}{2} \right) \right)$	$R_{so} \leq r \leq R_{sl}$ $ \theta - \theta_j \leq \frac{\delta}{2}$

Appendix B

The solutions for the integrals are given below:

$$\text{For } \alpha_r = \frac{xp}{t}$$

$$\rho_s(t, x, k) = -\frac{1}{4t\pi} \left[\cos\left(\frac{3x\pi}{2} + t\alpha + \frac{kt\pi}{p}\right) - \cos\left(\frac{x\pi}{2} - t\alpha - \frac{kt\pi}{p}\right) \right] - \frac{\alpha_r}{2p} \sin\left(\frac{x\pi}{2} - t\alpha - \frac{kt\pi}{p}\right) \dots (30)$$

$$\rho_c(t, x, k) = \frac{1}{4t\pi} \left[\sin\left(\frac{3x\pi}{2} + t\alpha + \frac{kt\pi}{p}\right) + \sin\left(\frac{x\pi}{2} - t\alpha - \frac{kt\pi}{p}\right) \right] - \frac{\alpha_r}{2p} \cos\left(\frac{x\pi}{2} - t\alpha - \frac{kt\pi}{p}\right) \dots (31)$$

$$6_s(t, x, k) = -\frac{1}{2t\pi} \left[\sin\left(\frac{3x\pi}{2} + t\alpha + \frac{kt\pi}{p}\right) + \sin\left(\frac{x\pi}{2} - t\alpha - \frac{kt\pi}{p}\right) \right] - \cos\left(\frac{x\pi}{2} - t\alpha - \frac{kt\pi}{p}\right) \dots (32)$$

$$6_c(t, x, k) = -\frac{1}{2t\pi} \left[\cos\left(\frac{3x\pi}{2} + t\alpha + \frac{kt\pi}{p}\right) - \cos\left(\frac{x\pi}{2} - t\alpha - \frac{kt\pi}{p}\right) \right] + \sin\left(\frac{x\pi}{2} - t\alpha - \frac{kt\pi}{p}\right) \dots (33)$$

And for $\alpha_r \neq \frac{xp}{t}$ we have:

$$\rho_s(t, x, k) = \frac{\alpha_r}{2\pi} \left\{ \frac{-\cos\left(x\pi + \frac{t\pi\alpha_r}{2p} + t\alpha + \frac{kt\pi}{p}\right) + \cos\left(\frac{t\pi\alpha_r}{2p} - t\alpha - \frac{kt\pi}{p}\right)}{\alpha_r t + xp} - \frac{\cos\left(x\pi - \frac{t\pi\alpha_r}{2p} - t\alpha - \frac{kt\pi}{p}\right) - \cos\left(\frac{t\pi\alpha_r}{2p} - t\alpha - \frac{kt\pi}{p}\right)}{\alpha_r t + xp} \right\} \dots (34)$$

$$\rho_c(t, x, k) = \frac{\alpha_r}{2\pi} \left\{ \frac{-\cos\left(x\pi + \frac{t\pi\alpha_r}{2p} + t\alpha + \frac{kt\pi}{p}\right) + \cos\left(\frac{t\pi\alpha_r}{2p} - t\alpha - \frac{kt\pi}{p}\right)}{\alpha_r t + xp} - \frac{\cos\left(x\pi - \frac{t\pi\alpha_r}{2p} - t\alpha - \frac{kt\pi}{p}\right) - \cos\left(\frac{t\pi\alpha_r}{2p} - t\alpha - \frac{kt\pi}{p}\right)}{\alpha_r t + xp} \right\} \dots (35)$$

$$6_s(t, x, k) = \frac{p}{\pi} \left\{ \frac{-\sin\left(x\pi + \frac{t\pi\alpha_r}{2p} + t\alpha + \frac{kt\pi}{p}\right) - \sin\left(\frac{t\pi\alpha_r}{2p} - t\alpha - \frac{kt\pi}{p}\right)}{\alpha_r t + xp} - \frac{\sin\left(x\pi - \frac{t\pi\alpha_r}{2p} - t\alpha - \frac{kt\pi}{p}\right) - \sin\left(\frac{t\pi\alpha_r}{2p} - t\alpha - \frac{kt\pi}{p}\right)}{\alpha_r t + xp} \right\} \dots (36)$$

$$6_c(t, x, k) = \frac{p}{\pi} \left\{ \frac{-\cos\left(x\pi + \frac{t\pi\alpha_r}{2p} + t\alpha + \frac{kt\pi}{p}\right) + \cos\left(\frac{t\pi\alpha_r}{2p} - t\alpha - \frac{kt\pi}{p}\right)}{\alpha_r t + xp} + \frac{\cos\left(x\pi - \frac{t\pi\alpha_r}{2p} - t\alpha - \frac{kt\pi}{p}\right) - \cos\left(\frac{t\pi\alpha_r}{2p} - t\alpha - \frac{kt\pi}{p}\right)}{\alpha_r t + xp} \right\} \dots (37)$$

For $\pi z \neq \beta t$

$$\mathcal{E}_s(t, z, j) = 2\pi z \frac{(-1)^{z+1} \sin\left(t\left(\theta_j + \frac{\beta}{2}\right)\right) + \sin\left(t\left(\theta_j - \frac{\beta}{2}\right)\right)}{\pi^2 z^2 - \beta^2 t^2} \dots (38)$$

$$\mathcal{E}_c(t, z, j) = 2\pi z \frac{(-1)^{z+1} \cos\left(t\left(\theta_j + \frac{\beta}{2}\right)\right) + \cos\left(t\left(\theta_j - \frac{\beta}{2}\right)\right)}{\pi^2 z^2 - \beta^2 t^2} \dots (39)$$

$$\eta_s(t, z, j) = \frac{\beta^2 t}{\pi} \frac{(-1)^z \cos\left(t\left(\theta_j + \frac{\beta}{2}\right)\right) - \cos\left(t\left(\theta_j - \frac{\beta}{2}\right)\right)}{\pi^2 z^2 - \beta^2 t^2} \dots (40)$$

$$\eta_c(t, z, j) = \frac{\beta^2 t}{\pi} \frac{(-1)^{z+1} \sin\left(t\left(\theta_j + \frac{\beta}{2}\right)\right) + \sin\left(t\left(\theta_j - \frac{\beta}{2}\right)\right)}{\pi^2 z^2 - \beta^2 t^2} \dots (41)$$

And for $\pi z = \beta t$ we have:

$$\mathcal{E}_s(t, z, j) = \cos\left(t\left(\theta_j - \frac{\beta}{2}\right)\right) - \frac{\sin\left(t\left(\theta_j + \frac{\beta}{2}\right)\right) - \sin\left(t\left(\theta_j - \frac{\beta}{2}\right)\right)}{2t\beta} \dots (42)$$

$$\mathcal{E}_c(t, z, j) = -\sin\left(t\left(\theta_j - \frac{\beta}{2}\right)\right) - \frac{\cos\left(t\left(\theta_j + \frac{\beta}{2}\right)\right) - \cos\left(t\left(\theta_j - \frac{\beta}{2}\right)\right)}{4t\pi} \dots (43)$$

$$\eta_s(t, z, j) = \frac{-\sin\left(t\left(\theta_j - \frac{\beta}{2}\right)\right)}{\frac{2\pi}{\beta}} - \frac{\cos\left(t\left(\theta_j + \frac{\beta}{2}\right)\right) - \cos\left(t\left(\theta_j - \frac{\beta}{2}\right)\right)}{4t\pi} \dots (44)$$

$$\eta_c(t, z, j) = \frac{\cos\left(t\left(\theta_j - \frac{\beta}{2}\right)\right)}{\frac{2\pi}{\beta}} + \frac{\sin\left(t\left(\theta_j + \frac{\beta}{2}\right)\right) - \sin\left(t\left(\theta_j - \frac{\beta}{2}\right)\right)}{4t\pi} \dots (45)$$

For $\delta \neq \frac{\beta y}{z}$

$$\gamma_s(z, y) = \frac{2\delta^2 z}{\pi} \frac{(-1)^{z+1} \sin\left(\frac{\pi y}{2\delta}(\delta + \beta)\right) + \sin\left(\frac{\pi y}{2\delta}(\delta - \beta)\right)}{\delta^2 z^2 - \beta^2 y^2} \dots (46)$$

$$\gamma_c(z, y) = \frac{2\beta^2 y}{\pi} \frac{(-1)^{z+1} \sin\left(\frac{\pi y}{2\delta}(\delta + \beta)\right) + \sin\left(\frac{\pi y}{2\delta}(\delta - \beta)\right)}{\delta^2 z^2 - \beta^2 y^2} \dots (47)$$

And for $\delta = \frac{\beta y}{z}$ we have:

$$\gamma_s(z, y) = \frac{2\pi z \cos\left(\frac{\pi}{2}(z-y)\right) - \sin\left(\frac{\pi}{2}(3z+y)\right) - \sin\left(\frac{\pi}{2}(z-y)\right)}{2\pi z} \dots (48)$$

$$\gamma_c(z, y) = \frac{2\pi z \cos\left(\frac{\pi}{2}(z-y)\right) + \sin\left(\frac{\pi}{2}(3z+y)\right) + \sin\left(\frac{\pi}{2}(z-y)\right)}{2\pi z} \dots (49)$$

$$\xi_{x1}^k = \xi_{x3}^k = -\mu_0 \left[\frac{M_{Rx}^k - \frac{xp}{\alpha_r} M_{Tx}^k}{\left(\frac{xp}{\alpha_r}\right)^2 - 1} \right] \dots (50)$$

$$\xi_{x2}^k = -\mu_0 \left[\frac{\frac{xp}{\alpha_r} M_{Rx}^k - M_{Tx}^k}{\left(\frac{xp}{\alpha_r}\right)^2 - 1} \right] \dots (51)$$

Internal Rotor Machine:

The simultaneous equations for integral constant calculations are summarized as following matrix (for PM & AR):

$$\begin{bmatrix} A^{11} & A^{12} & A^{13} & A^{14} & A^{14} & 0 & 0 & 0 \\ A^{21} & A^{22} & A^{23} & 0 & 0 & 0 & 0 & 0 \\ 0 & A^{32} & A^{33} & 0 & 0 & A^{36} & A^{37} & 0 \\ A^{41} & 0 & 0 & A^{44} & A^{45} & 0 & 0 & 0 \\ 0 & 0 & 0 & A^{54} & A^{55} & A^{56} & A^{57} & 0 \\ 0 & A^{62} & A^{63} & 0 & A^{64} & A^{65} & A^{66} & A^{67} \\ 0 & 0 & 0 & 0 & 0 & A^{76} & A^{77} & A^{78} \\ 0 & 0 & 0 & 0 & 0 & A^{86} & A^{87} & A^{88} \end{bmatrix} \begin{bmatrix} a^m \\ a^a \\ b^a \\ c^a \\ d^a \\ a^{so} \\ b^{so} \\ b^{sl} \end{bmatrix} = \begin{bmatrix} \Gamma^{1,PM} \\ \Gamma^{1,PM} \\ \Gamma^{1,AR} \\ \Gamma^{1,PM} \\ \Gamma^{1,AR} \\ 0 \\ \Gamma^{1,AR} \\ \Gamma^{1,AR} \end{bmatrix}$$

The elements of the simultaneous equations for non-overlapping consequent-pole are as follows:

$$A_{x,x}^{11} = \bar{x} \left[1 + \left(\frac{R_r}{R_m}\right)^{2\bar{x}} \right] \dots (52)$$

Where $\bar{x} = \frac{xp}{\alpha_r}$

$$A_{x+kx,t}^{12} = -t \left(\frac{R_m}{R_s}\right)^t 6_s(t, x, k) \dots (53)$$

$$A_{x+kx,t}^{13} = -t 6_s(t, x, k) \dots (54)$$

$$A_{x+kx,t}^{14} = t \left(\frac{R_m}{R_s}\right)^t 6_c(t, x, k) \dots (55)$$

$$A_{x+kx,t}^{15} = t 6_c(t, x, k) \dots (56)$$

$$\Gamma_{x+kx,1}^{1,PM} = -R_m \bar{x} \left[\xi_{x1}^k \left(\frac{R_r}{R_m}\right)^{\bar{x}+1} + \xi_{x1}^k \right] \dots (57)$$

$$A_{t,x+kx}^{21} = \frac{\bar{x}}{\mu_r} \left[\left(\frac{R_r}{R_m}\right)^{2\bar{x}} - 1 \right] \rho_c(t, x, k) \dots (58)$$

$$A_{t,t}^{22} = t \left(\frac{R_m}{R_s}\right)^t \dots (59)$$

$$A_{t,t}^{23} = -t \dots (60)$$

$$\Gamma_{t,1}^{2,PM} = \sum_{k=0}^{p-1} \sum_{x=1}^X \frac{\bar{x}}{\mu_r} R_m \left[-\xi_{x1}^k \left(\frac{R_r}{R_m}\right)^{\bar{x}+1} + \xi_{x3}^k \right] \rho_c(n, w, k) \dots (61)$$

$$A_{t,t}^{32} = t \dots (62)$$

$$A_{t,t}^{33} = -t \left(\frac{R_m}{R_s}\right)^t \dots (63)$$

$$A_{t,z}^{36} = -\bar{z} \left(\frac{R_s}{R_{so}}\right)^{\bar{z}} \eta_c(t, z, j) \dots (64)$$

Where $\bar{z} = \frac{zp}{\alpha_r}$

$$A_{t,z}^{36} = \bar{u} \eta_c(t, z, j) \dots (65)$$

$$\Gamma_{t,1}^{3,AR} = \sum_{j=0}^Q \eta_c(t, 0, j) b_0^{so,j} \dots (66)$$

$$A_{t,x+kx}^{41} = \frac{\bar{x}}{\mu_r} \left[\left(\frac{R_r}{R_m}\right)^{2\bar{x}} - 1 \right] \rho_s(t, x, k) \dots (67)$$

$$A_{t,t}^{44} = t \left(\frac{R_m}{R_s}\right)^t \dots (68)$$

$$A_{t,t}^{45} = -t \dots (69)$$

$$\Gamma_{t,1}^{4,PM} = \sum_{k=0}^{p-1} \sum_{x=1}^X \frac{\bar{x}}{\mu_r} R_m \left[-\xi_{x1}^k \left(\frac{R_r}{R_m}\right)^{\bar{x}+1} + \xi_{x3}^k \right] \rho_s(t, x, k) \dots (70)$$

$$A_{t,t}^{54} = t \dots (71)$$

$$A_{t,t}^{55} = -t \left(\frac{R_m}{R_s}\right)^t \dots (72)$$

$$A_{t,z}^{56} = -\bar{z} \left(\frac{R_s}{R_{so}}\right)^{\bar{z}} \eta_s(t, z, j) \dots (73)$$

$$A_{t,z}^{57} = \bar{u} \eta_s(n, u, j) \dots (74)$$

$$\Gamma_{t,1}^{5,AR} = \sum_{j=0}^Q \eta_s(t, 0, j) b_0^{so,j} \dots (75)$$

$$A_{t,t}^{62} = -t \mathcal{E}_s(t, z, j) \dots (76)$$

$$A_{z,t}^{63} = -t \left(\frac{R_m}{R_s}\right)^t \mathcal{E}_s(t, z, j) \dots (77)$$

$$A_{t,t}^{64} = t \mathcal{E}_c(t, z, j) \dots (78)$$

$$A_{z,t}^{65} = t \left(\frac{R_m}{R_s}\right)^t \mathcal{E}_c(t, z) \dots (79)$$

$$A_{t,z}^{66} = \bar{z} \left(\frac{R_s}{R_{so}}\right)^{\bar{z}} \dots (80)$$

$$A_{z,z}^{67} = \bar{z} \dots (81)$$

$$A_{z,z}^{76} = \bar{z} \dots (82)$$

$$A_{z,z}^{77} = \bar{z} \left(\frac{R_s}{R_{so}}\right)^{\bar{z}} \dots (83)$$

$$A_{x,x}^{78} = -\bar{y} \left[\left(\frac{R_{so}}{R_{sl}}\right)^{2\bar{y}} + 1 \right] \gamma_c(z, y) \dots (84)$$

Where $\bar{y} = \frac{yp}{\alpha_r}$

$$\Gamma_{y,1}^{7,AR} = \sum_{y=1}^Y \frac{\mu_0 J_v^j}{\bar{u}^2 - 4} \left[\bar{u} R_{so}^2 - 2 R_{sl}^2 \left(\frac{R_{so}}{R_{sl}}\right)^{\bar{y}} \right] \gamma_s(z, y) \dots (85)$$

$$A_{y,z}^{86} = -\bar{z} \gamma_c(z, y) \dots (86)$$

$$A_{y,z}^{87} = \bar{z} \left(\frac{R_s}{R_{so}}\right)^{\bar{z}} \gamma_c(z, y) \dots (87)$$

$$A_{y,y}^{88} = \bar{y} \left[\left(\frac{R_{so}}{R_{sl}}\right)^{2\bar{y}} - 1 \right] \dots (88)$$

$$\Gamma_{y,1}^{8,AR} = \frac{-2\mu_0 J_v^j}{\bar{y}^2 - 4} \left[R_{so}^2 - 2 R_{sl}^2 \left(\frac{R_{so}}{R_{sl}}\right)^{\bar{y}} \right] + \gamma_c(0, v) b_0^{so,j} \dots (89)$$

$$b_0^{so,j} = \frac{\mu_0 J_0^j}{2} [R_{sl}^2 - R_{so}^2] \frac{\delta}{\beta} \dots (90)$$

External Rotor Machine:

- Due to **PM**:

$$\begin{bmatrix} C & D \\ F & F \end{bmatrix} \begin{bmatrix} a^a \\ a^m \end{bmatrix} = \begin{bmatrix} g \\ h \end{bmatrix}$$

Where

$$C_{i,i} = yp \left[\left(\frac{R_m}{R_s}\right)^{2yp} - 1 \right] \dots (91)$$

$$D_{i,j} = yp \left[\left(\frac{R_r}{R_m}\right)^{\frac{2yp}{\alpha_r}} - 1 \right] (H_{yt}^+ - H_{yt}^-) \dots (92)$$

$$E_{j,i} = yp \left[\left(\frac{R_m}{R_s}\right)^{\frac{2yp}{\alpha_r}} + 1 \right] (H_{yt}^+ + H_{yt}^-) \dots (93)$$

$$F_{j,j} = -\frac{\mu_r yp}{\alpha_r} \left[\left(\frac{R_r}{R_m}\right)^{\frac{2yp}{\alpha_r}} + 1 \right] \dots (94)$$

$$g_i = \sum_{t=1}^T tp \left[\left(\frac{R_m}{R_s}\right)^{\frac{2yp}{\alpha_r}} \right] (H_{yt}^+ - H_{yt}^-) \dots (95)$$

$$h_j = \mu_r \left[\left(\frac{R_r}{R_m}\right)^{\frac{2yp}{\alpha_r} + 1} - \frac{M_{Rt}^k}{\mu_r} \right] \dots (96)$$

$$H_{yt}^+ = \frac{\sin(\alpha_r y + t)}{(\alpha_r y + t)}, H_{yt}^- = \frac{\sin(\alpha_r y - t)}{(\alpha_r y - t)} \dots (97)$$

- Due to **AR**:

$$\begin{bmatrix} A^{11} & 0 & A^{13} & A^{14} \\ 0 & A^{22} & A^{23} & A^{24} \\ A^{31} & A^{32} & A^{33} & 0 \\ A^{41} & A^{42} & 0 & A^{44} \end{bmatrix} \begin{bmatrix} b^w \\ d^w \\ a^{m,0} \\ a^{m,1} \end{bmatrix} = \begin{bmatrix} \Gamma^1 \\ \Gamma^2 \\ \Gamma^3 \\ \Gamma^4 \end{bmatrix}$$

$$A_{t,t}^{11} = 2t \left[\left(\frac{R_m}{R_s} \right)^{2tp} - 1 \right] \dots (98)$$

$$A_{t,y}^{13} = \frac{y}{\mu_r \alpha_r} \left[\left(\frac{R_r}{R_m} \right)^{\frac{2tp}{\alpha_r}} - 1 \right] \mathcal{E}_s(t, y) \dots (99)$$

$$A_{t,y}^{14} = (-1)^t \frac{y}{\mu_r \alpha_r} \left[\left(\frac{R_r}{R_m} \right)^{\frac{2tp-1}{\alpha_r}} - 1 \right] \mathcal{E}_s(t, y) \dots (100)$$

$$\Gamma_t^1 = 2t \left[\xi_{t1}^k \left(\frac{R_m}{R_s} \right)^{tp-1} - \frac{\xi_{t2}^k + \xi_{t3}^k}{2} \left(\frac{R_m}{R_a} \right)^{tp-1} + \frac{\xi_{t2}^k - \xi_{t3}^k}{2} \left(\frac{R_a}{R_m} \right)^{tp+1} \right] \dots (101)$$

$$A_{t,t}^{22} = 2t \left[\left(\frac{R_m}{R_s} \right)^{2tp} - 1 \right] \dots (102)$$

$$A_{t,y}^{23} = \frac{y}{\mu_r \alpha_r} \left[\left(\frac{R_r}{R_m} \right)^{\frac{2tp}{\alpha_r}} - 1 \right] \mathcal{E}_c(t, y) \dots (103)$$

$$A_{t,y}^{24} = (-1)^t \frac{y}{\mu_r \alpha_r} \left[\left(\frac{R_r}{R_m} \right)^{\frac{2tp-1}{\alpha_r}} - 1 \right] \mathcal{E}_c(t, y) \dots (104)$$

$$\Gamma_t^2 = 2t \left[\xi_{t1}^k \left(\frac{R_m}{R_s} \right)^{tp-1} - \frac{\xi_{t2}^k + \xi_{t3}^k}{2} \left(\frac{R_m}{R_a} \right)^{tp-1} + \frac{\xi_{t2}^k - \xi_{t3}^k}{2} \left(\frac{R_a}{R_m} \right)^{tp+1} \right] \dots (105)$$

$$A_{y,t}^{31} = t \left[\left(\frac{R_m}{R_s} \right)^{2tp} + 1 \right] \gamma_c(t, y) \dots (106)$$

$$A_{y,t}^{32} = -t \left[\left(\frac{R_m}{R_s} \right)^{2tp} + 1 \right] \gamma_s(t, y) \dots (107)$$

$$A_{y,y}^{33} = \frac{y}{\alpha_r} \left[\left(\frac{R_r}{R_m} \right)^{\frac{2tp}{\alpha_r}} - 1 \right] \dots (108)$$

$$\Gamma_y^3 = \sum_{t=1}^T t \left\{ \left[\xi_{t1}^k \left(\frac{R_m}{R_s} \right)^{tp-1} - \frac{\xi_{t2}^k + \xi_{t3}^k}{2} \left(\frac{R_m}{R_a} \right)^{tp-1} + \frac{\xi_{t2}^k - \xi_{t3}^k}{2} \left(\frac{R_a}{R_m} \right)^{tp+1} \right] \gamma_c(t, y) - \left[\xi_{t1}^k \left(\frac{R_m}{R_s} \right)^{tp-1} - \frac{\xi_{t2}^k + \xi_{t3}^k}{2} \left(\frac{R_m}{R_a} \right)^{tp-1} + \frac{\xi_{t2}^k - \xi_{t3}^k}{2} \left(\frac{R_a}{R_m} \right)^{tp+1} \right] \gamma_s(t, y) \right\} \dots (109)$$

$$A_{y,t}^{41} = (-1)^t t \left[\left(\frac{R_m}{R_s} \right)^{2tp} + 1 \right] \gamma_c(t, y) \dots (110)$$

$$A_{y,t}^{42} = (-1)^{t+1} t \left[\left(\frac{R_m}{R_s} \right)^{2tp} + 1 \right] \gamma_s(t, y) \dots (111)$$

$$A_{t,y}^{44} = \frac{y}{\alpha_r} \left[\left(\frac{R_r}{R_m} \right)^{\frac{2tp}{\alpha_r}} - 1 \right] \dots (112)$$

$$\Gamma_y^4 = \sum_{t=1}^T (-1)^t t \left\{ \left[\xi_{t1}^k \left(\frac{R_m}{R_s} \right)^{tp-1} - \frac{\xi_{t2}^k + \xi_{t3}^k}{2} \left(\frac{R_m}{R_a} \right)^{tp-1} + \frac{\xi_{t2}^k - \xi_{t3}^k}{2} \left(\frac{R_a}{R_m} \right)^{tp+1} \right] \gamma_c(t, y) - \left[\xi_{t1}^k \left(\frac{R_m}{R_s} \right)^{tp-1} - \frac{\xi_{t2}^k + \xi_{t3}^k}{2} \left(\frac{R_m}{R_a} \right)^{tp-1} + \frac{\xi_{t2}^k - \xi_{t3}^k}{2} \left(\frac{R_a}{R_m} \right)^{tp+1} \right] \gamma_s(t, y) \right\} \dots (113)$$

Appendix C

Table VI A summary of the references published on the analytical modeling of brushless permanent magnet machines.

Reference	Year	Movement	Flux Direction	Stator Structure	Magnet Configuration SM/SI	Magnetization Pattern	Number of Dimension	Coordinate	Magnetic Potential	Field due to AR/PM	Consideration & Calculation
[1]	1984	Rotary	Radial	Sd	SM	Radial	2-D	Ca	Vr	AR, PM	B (Infinite Back-Iron Permeability)
[2]	1985	Rotary	Radial	Ss	SM	Radial, Parallel	2-D	Po	Sr	PM	B (Infinite Back-Iron Permeability)
[3]	1989	Linear	-	Sd	SM	-	2-D, 3-D	Ca	Sr	AR, PM	Magnetic field distribution, MMF (Infinite Back-Iron Permeability)
[4]	1992	Rotary	Radial	Sd	SM	Radial	2-D	Cylindrical	Sr	PM	CT (Infinite Back-Iron Permeability)
[5]-[6]	1993	Rotary	Radial	Sd, Ss	SM	Radial	1-D, 2-D	Po	Sr	AR, PM	B (Infinite Back-Iron Permeability)
[7]	2010	Rotary	Radial	Sd	SM	Radial	2-D	Po	Vr	AR, PM	P _e (Infinite Back-Iron Permeability)
[8]	1993	Rotary	Radial	Sd, Ss	SM	Radial	1-D, 2-D	Po	Sr	AR, PM	B (Infinite Back-Iron Permeability)
[9]	2000	Rotary	Radial	Ss	SM	Sinusoidal amplitude magnetization	2-D	Po	Vr, Sr	PM	B (Infinite Back-Iron Permeability)
[10]	2000	Rotary	Radial	Sd	SM	Parallel, 6-segmented magnet in shifting direction	2-D	Ca	Vr	AR, PM	B, Eddy current losses
[11]	2001	Linear	-	Ss	SM	Parallel	2-D	Ca	Vr	AR, PM	e (Infinite Back-Iron Permeability)
[12]	2002	Rotary	Radial	Sd, Ss	SM	Radial, Parallel	2-D	Po	Sr	AR, PM	B, (Infinite Core Permeability)
[13]	2003	Rotary	Radial	Sd	SM	Radial	1-D, 2-D	Po	Vr, Sr	AR, PM	B (Infinite Back-Iron Permeability)





Reference	Year	Movement	Flux Direction	Stator Structure	Magnet Configuration SM/SI	Magnetization Pattern	Number of Dimension	Coordinate	Magnetic Potential	Field due to AR/PM	Consideration & Calculation
[14]	2003	Rotary	Radial	Sd	SM	Radial	2-D	Po	Sr	AR, PM	B, e (Infinite Core Permeability)
[15]	2004	Rotary	Radial	Sd	SM	-	-	Ca	-	PM	B, CT
[16]	2004	Rotary	Radial, Axial	Ss	SM	-	2-D	Po	Vr	AR	B, Eddy current (Infinite Back-Iron Permeability)
[17]	2004	Rotary	Radial	Ss	SM	Ideal Halbach	2-D	Po	Sr	PM	B (Infinite Back-Iron Permeability)
[18]	2000	Rotary	Radial	Sd	SM	Radial	2-D	Po	Vr	AR, PM	Eddy current losses, MMF (Infinite Back-Iron Permeability)
[19]	2008	Rotary	Radial	Sd, Ss	SM	Radial, Parallel, Sinusoidal amplitude magnetization, Ideal Halbach	2-D	Po	Vr	PM	B, CT, e (Infinite Back-Iron Permeability)
[20]	2006	Rotary	Radial	Sd	SM	Radial, Parallel	2-D	Po	Sr	PM	B, CT, e (Infinite Back-Iron Permeability)
[21]	2008	Rotary	Radial	Sd	SM	Radial	2-D	Po	Vr	PM	B, CT (Infinite Back-Iron Permeability)
[22]	2009	Rotary	Radial	Sd	SM	Nine-segment Halbach	2-D	Po	Vr	PM	B distribution, C, e, Electromagnetic T (Infinite Core Permeability)
[23]	2007	Linear	-	Sd	SM	Parallel	2-D	Ca	Sr	PM	B (Infinite Back-Iron Permeability)
[24]	2008	Rotary	Radial	Sd	SM	Radial	2-D	Po, Ca	Sr	PM	CT, UMF (Infinite Core Permeability)
[25]	2009	Rotary	Radial	Sd	SM	-	2-D	Po	Vr	AR	AR magnetic field (Infinite Back-Iron Permeability)
[26]	2009	Rotary	Radial	Sd	SM	Radial, Parallel	2-D	Po	Vr	PM	No-load magnetic field distribution (Infinite Back-Iron Permeability)

Reference	Year	Movement	Flux Direction	Stator Structure	Magnet Configuration SM/SI	Magnetization Pattern	Number of Dimension	Coordinate	Magnetic Potential	Field due to AR/PM	Consideration & Calculation
[27]	2011	Rotary	Radial	Sd	SM	Radial	2-D	Po	Vr	AR, PM	Magnetic field distribution (Infinite Back-Iron Permeability)
[28]	2011	Rotary	Radial	Sd	SM	-	2-D	Po	Vr	AR	AR field (Infinite Back-Iron Permeability)
[29]	2011	Rotary	Radial	Sd	SM	Radial, Parallel	2-D	Po	Vr	PM	Open-circuit magnetic field distribution (Infinite Core Permeability)
[30]	2010	Rotary	Radial	Sd	SM	Radial, Parallel	2-D	Po	Sr	PM	Magnetic field distribution, e, Electromagnetic T, CT (Infinite Core Permeability)
[31]	2012	Rotary	Radial	Sd	SM	Radial, Parallel	2-D	Po	Sr	AR, PM	B, CT, e, Electromagnetic torque, Saturation effect (Infinite Core Permeability)
[32]	2020	Linear	-	Ss	SM	Parallel	0-D,2-D	Po	Vr	PM	B, L (Infinite Iron Core Permeability)
[33]	1993	Rotary	Radial	Sd, Ss	SM	Radial	1-D, 2-D	Po	Sr	AR, PM	B (Infinite Back-Iron Permeability)
[34]	2016	Rotary	Radial	Ss	-	-	3-D	Cylindrical	Vr	AR	Magnetic field distribution, Pe (Infinite Back-Iron Permeability)
[35]	2017	Linear	-	Sd	SM	-	2-D, 3-D	Ca	Vr	AR	Ar field distribution, L (Infinite Back-Iron Permeability)
[36]	2017	Linear	-	Sd, Ss	SM	parallel	2-D	Ca	Sr	AR, PM	e (Infinite core Permeability)
[37]	2019	Linear	-	Ss	SM	Radial, Parallel	3-D	Cylindrical	Sr	PM	T, Field Distribution (Infinite core Permeability)



Reference	Year	Movement	Flux Direction	Stator Structure	Magnet Configuration SM/SI	Magnetization Pattern	Number of Dimension	Coordinate	Magnetic Potential	Field due to AR/PM	Consideration & Calculation
[38]	2020	Rotary	Axial	Sd	-	Radial	3-D	Po	Sr	PM	B, e, CT (Static Radial Deviation & Angular Eccentricity)
[39]	2009	Rotary	Radial	Sd	SI	Radial	2-D	Po	Sr	PM	Magnetic field distribution (Infinite Back-Iron Permeability)
[40]	2013	Rotary	Radial	Ss	SI	Radial, Parallel, Halbach	2-D	Po	Vr	AR, PM	Electromagnetic T, Reluctance T, L, e (Infinite Core Permeability)
[41]	2012	Rotary	Radial	Sd	SI	Radial	2-D	Po	Vr	AR, PM	Magnetic field distribution (Infinite Back-Iron Permeability)
[42]	2013	Rotary	Radial	Ss	SI	Radial, Parallel, Sinusoidal amplitude magnetization, Ideal Halbach, Halbach	2-D	Po	Vr	AR, PM	Open-circuit magnetic field distribution (Finite Core Permeability)
[43]	2013	Rotary	Radial, Axial	Sd	SI	Radial, Parallel	2-D	Ca	Vr	AR, PM	Magnetic flux distribution, Instantaneous T (Infinite Back-Iron Permeability)
[44]	2004	Rotary	Axial	Sd	SM	-	2-D, 3-D	Po, Ca	Vr	AR, PM	B (Infinite Back-Iron Permeability)
[45]	2004	Rotary	Radial	Sd	SM	Radial	2-D	Po	Vr	AR, PM	T, Magnetic Force (Infinite Core Permeability)
[46]	2005	Rotary	Radial	Sd	SM	-	2-D	Po	Vr	AR	Magnetic field distribution, Eddy-current loss, MMF (Infinite Core Permeability)
[47]	2005	Rotary	Axial	Sd	SM	Parallel	3-D	Po	Vr	PM	CT (Infinite Back-Iron Permeability)
[48]	2005	Rotary	Radial	Sd, Ss	SM	Parallel	2-D	Po	Vr	AR, PM	B, CT, Pe (Infinite Core Permeability)



Reference	Year	Movement	Flux Direction	Stator Structure	Magnet Configuration SM/SI	Magnetization Pattern	Number of Dimension	Coordinate	Magnetic Potential	Field due to AR/PM	Consideration & Calculation
[49]	2018	Linear Tubular	Radial	Sd	BPM	-	2-D	Ca	Sr	AR, PM	B, CT, Cogging force
[50]	2018	Rotary-Linear	Radial	Sd	BPM	-	2-D	Ca, Po	Sr	AR, PM	B, λ
[51]	2018	Linear	-	Ss	SM	Two-segment Halbach, Parallel	2-D	Ca	Vr	AR, PM	B distribution, λ , e (Finite core Permeability)
[52]	2011	Rotary	Radial	Ss	SI	Radial, Parallel, Halbach	2-D	Po	Sr	PM	Open-circuit magnetic field distribution (Infinite Back-Iron Permeability)
[53]	2012	Rotary	Radial	Ss	SM, SI	-	2-D	Po	Vr	AR	Ar field distribution (Infinite Back-Iron Permeability)
[54]	2012	Rotary	Radial	Sd	SI	Radial, Parallel, Halbach	2-D	Po	Vr	AR, PM	Magnetic field distribution (Infinite Core Permeability)
[55]	2015	Rotary	Radial	Sd	SM	Radial	2-D	Ca	Sr	AR, PM	Magnetic field distribution
[56]	2012	Rotary	Radial	Ss	SM	Radial, Parallel, Sinusoidal amplitude magnetization, Ideal Halbach, Halbach	2-D	Po	Vr	PM	Open-circuit magnetic field distribution, T (Infinite Back-Iron Permeability)
[57]	2010	Rotary, Linear, Tubular	Radial, Axial	Sd, Ss	SM	Radial, Parallel, Halbach	2-D	Po, Ca, Cylindrical	Vr	PM	Magnetic field distribution (Infinite Back-Iron Permeability)
[58]	1994	Rotary	Radial	Ss	SM, SI	Radial	2-D	Po	Sr	PM	B (Infinite Back-Iron Permeability)
[59]	1994	Rotary	Radial	Sd	SM	Radial	2-D	Po	Vr	PM	B (Infinite Back-Iron Permeability)
[60]	1995	Rotary	-	Sd	SM	-	2-D	Ca	Vr	AR	B, L, M (Infinite Back-Iron Permeability)

Reference	Year	Movement	Flux Direction	Stator Structure	Magnet Configuration SM/SI	Magnetization Pattern	Number of Dimension	Coordinate	Magnetic Potential	Field due to AR/PM	Consideration & Calculation
[61]	1995	Rotary	Radial	Ss	SM	Radial	-	Po	Vr	PM	ie and thermal problems (Finite Back-Iron Permeability)
[62]	1996	Rotary	Radial	Sd	SM	Radial, Parallel	2-D	Ca	Vr	PM	Time-varying field distribution (Infinite Core Permeability)
[63]	1997	Rotary	Radial	Ss	SM	-	2-D	Po	Vr, Sr	AR	Commutation losses (Finite Back-Iron Permeability)
[64]	1998	Rotary	Radial	Sd	SM	-	2-D	Po	Vr, Sr	AR	Pe (Finite Core Permeability)
[65]	1998	Rotary	Radial	Ss	SM	Radial	2-D	Po	Vr	PM	Instantaneous magnetic field distribution (Infinite Core Permeability)
[66]	1998	Rotary	Radial	Sd	SM	Radial	2-D	Po	Sr	PM	Magnetic field distribution (Infinite Back-Iron Permeability)
[67]	1998	Rotary	Radial	Ss	SM	-	2-D	Po	Vr	AR	AR field and winding inductance (Infinite Back-Iron Permeability)
[68]	1998	Rotary	Radial	Sd	SM	Radial	3-D	-	Vr	AR, PM	Magnetic field distribution (Infinite Back-Iron Permeability)
[69]	1999	Rotary	Radial	Ss	SM	Radial	2-D	Po	Vr	PM	Magnetic field distribution (Infinite Back-Iron Permeability)
[70]	1999	Rotary	Radial	Ss	SM	Radial, Parallel	2-D	Po	Vr, Sr	AR, PM	e, Field distribution, winding inductance, iron loss (Finite Back-Iron Permeability)
[71]	1999	Tubular, Linear	Radial, Axial	Sd, Ss	SM	Radial, Parallel, Halbach	2-D	Cylindrical	Vr	AR, PM	B (Infinite Back-Iron Permeability)

[72]	2006	Linear	-	Ss	SM	-	2-D	Ca	Vr	PM	Magnetic field distribution, Optimization (Infinite Core Permeability)
[73]	2009	Rotary, Linear	Axial	Sd	SM	-	-	Ca	Vr	PM	B, CT, Optimization (Infinite Core Permeability)
[74]	2010	Linear	-	Ss	SM	Parallel	2-D	Ca	Vr	PM	B distribution, e, Optimization (Infinite Back-Iron Permeability)
[75]	2010	Linear	-	Sd	SM	Parallel	3-D	Po, Ca	Vr	PM	B (Infinite Back-Iron Permeability)

REFERENCES

- [1] N. Boules, "Two-Dimensional Field Analysis of Cylindrical Machines with Permanent Magnet Excitation," *IEEE Transactions on Industry Application*, vol. IA-20, no. 5, pp. 1267-1277, 1984.
- [2] N. Boules, "Prediction of No-Load Flux Density Distribution in Permanent Magnet Machines," *IEEE Transactions on Industry Application*, vol. IA-21, no. 3, pp. 633-643, 1985.
- [3] G. Xiong and S. A. Nasar, "Analysis of Fields And Forces in A Permanent Magnet Linear Synchronous Machine Based on The Concept of Magnetic Charge," *IEEE Transactions on Magnetics*, vol. 25, no. 3, pp. 2713-2719, 1989.
- [4] Z. Q. Zhu and D. Howe, "Analytical Prediction of the Cogging Torque in Radial-Field Permanent Magnet Brushless Motors," *IEEE Transactions on Magnetics*, vol. 28, no. 2, pp. 1371-1374, 1992.
- [5] Z. Q. Zhu, D. Howe, E. Bolte and B. Ackermann "Instantaneous Magnetic Field Distribution in Brushless Permanent Magnet Dc Motors, Part I: Open-Circuit Field," *IEEE Transactions on Magnetics*, vol. 29, no. 1, pp. 124-135, 1993.
- [6] Z. Q. Zhu and D. Howe, "Instantaneous Magnetic Field Distribution in Brushless Permanent Magnet DC Motors, Part II: Armature-Reaction Field," *IEEE Transactions on Magnetics*, vol. 29, no. 1, pp. 136-142, 1993.
- [7] Y. Amara, P. Reghem and G. Barakat, "Analytical Prediction of Eddy-Current Loss in Armature Windings of Permanent Magnet Brushless AC Machines," *IEEE Transactions on Magnetics*, vol. 46, no. 8, pp. 3481-3484, 2010.
- [8] Z. Q. Zhu and D. Howe, "Instantaneous Magnetic Field Distribution in Brushless Permanent Magnet DC Motors, Part IV: Magnetic Field on Load," *IEEE Transactions on Magnetics*, vol. 29, no. 1, pp. 152-158, 1993.
- [9] K. F. Rasmussen, J. H. Davies, T. J. E. Miller, M. I. McGilp and M. Olaru, "Analytical and Numerical Computation of Air-Gap Magnetic Fields in Brushless Motors with Surface Permanent Magnets," *IEEE Transactions on Industrial Application*, vol. 36, no. 6, pp. 1547-1554, 2000.
- [10] K. Yoshida, Y. Hita and K. Kesamaru, "Eddy-current loss analysis in PM of surface-mounted-PM SM for electric vehicles," *IEEE Transactions on Magnetics*, vol. 36, no. 4, pp. 1941-1944, 2000.
- [11] G. H. Kang, J. P. Hong and G. T. Kim, "A Novel Design of an Air-Core Type Permanent Magnet Linear Brushless Motor by Space Harmonics Field Analysis," *IEEE Transactions on Magnetics*, vol. 37, no. 5, pp. 3732 - 3736, 2001.
- [12] Z. Q. Zhu, D. Howe and C. C. Chan, "Improved Analytical Model for Predicting the Magnetic Field Distribution in Brushless Permanent-Magnet Machines," *IEEE Transactions on Magnetics*, vol. 38, no.1, pp. 229-238, 2002.
- [13] A. B. Proca, A. Keyhani, A. EL-Antably and W. Lu, "Analytical Model for Permanent Magnet Motors with Surface Mounted Magnets," *IEEE Transactions on Energy Conversion*, vol. 18, no. 3, pp. 386-391, 2003.
- [14] X. Wang, Q. Li and S. Wang, "Analytical Calculation of Air-Gap Magnetic Field Distribution and Instantaneous Characteristics of Brushless DC Motors," *IEEE Transactions on Energy Conversion*, vol. 18, no. 3, pp. 424-432, 2003.
- [15] J. F. Gieras, "Analytical Approach to Cogging Torque Calculation in PM Brushless Motors," *IEEE Transactions on Industry Application*, vol. 40, no. 5, pp. 3238-3240, 2004.
- [16] Z. Q. Zhu, K. Ng, N. Schofield and D. Howe, "Improved Analytical Modelling of Rotor Eddy Current Loss in Brushless Machines Equipped with Surface-Mounted Permanent Magnets," *IEEE Proceedings Electric Power Application*, vol. 151, no. 6, pp. 641-650, 2004.
- [17] Z. P. Xia, Z. Q. Zhu and D. Howe, "Analytical Magnetic Field Analysis of Halbach Magnetized Permanent-Magnet Machines," *IEEE Transactions on Magnetics*, vol. 40, no. 4, pp. 1864-1872, 2004.
- [18] K. Atallah, D. Howe, P. H. Mellor and D. A. Stone, "Rotor Loss in Permanent-Magnet Brushless AC Machines," *IEEE Transactions on Industry Applications*, vol. 36, no. 6, pp. 1612-1618, 2000.
- [19] P. Kumar and P. Bauer, "Improved Analytical Model of a Permanent-Magnet Brushless DC Motor," *IEEE Transactions on Magnetics*, vol. 44, no. 10, pp. 2299-2309, 2008.
- [20] D. Zarko, D. Ban and T. A. Lipo, "Analytical Calculation of Magnetic Field Distribution in the Slotted Air Gap of a Surface Permanent-Magnet Motor Using Complex Relative Air-Gap Permeance" *IEEE Transactions on Magnetics*, vol. 42, no. 7, pp. 1828-1837, 2006.
- [21] D. Zarko, D. Ban D and T. A. Lipo, "Analytical Solution for Cogging Torque in Surface Permanent-Magnet Motors Using Conformal Mapping," *IEEE Transactions on Magnetics*, vol. 44, no. 1, pp. 352-365, 2008.
- [22] K. Boughrara, B. L. Chikouche, R. Ibtouen, D. Zarko and O. Touhami, "Analytical Model of Slotted Air-Gap Surface Mounted Permanent-Magnet Synchronous Motor with Magnet Bars Magnetized in the Shifting Direction," *IEEE Transactions on Magnetics*, vol. 45, no. 2, pp. 747-758, 2009.
- [23] Z. J. Liu and J. T. Li, "Analytical Solution of Air-Gap Field in Permanent-Magnet Motors Taking Into Account the Effect of Pole Transition Over Slots," *IEEE Transactions on Magnetics*, vol. 43, no. 10, pp. 3872-3883, 2007.
- [24] Z. J. Liu and J. T. Li, "Accurate Prediction of Magnetic Field and Magnetic Forces in Permanent Magnet Motors Using an Analytical Solution," *IEEE Transactions on Energy Conversion*, vol. 23, no. 3, pp. 717-726, 2008.

- [25] Bellara, Y. Amara, G. Barakat and B. Dakyo, "Two-Dimensional Exact Analytical Solution of Armature Reaction Field in Slotted Surface Mounted PM Radial Flux Synchronous Machines," *IEEE Transactions on Magnetics*, vol. 45, no. 10, pp. 4534-4538, 2009.
- [26] F. Dubas and C. Espanet, "Analytical Solution of the Magnetic Field in Permanent Magnet Motors Taking Into Account Slotting Effect: No-Load Vector Potential and Flux Density Calculation," *IEEE Transactions on Magnetics*, vol. 45, no. 5, pp. 2097-2109, 2009.
- [27] T. Lubin, S. Mezani and A. Rezzoug, "2-D Exact Analytical Model for Surface-Mounted Permanent-Magnet Motors with Semi-Closed Slots" *IEEE Transactions on Magnetics*, vol. 47, no. 2, pp. 479-492, 2011.
- [28] L. J. Wu, Z. Q. Zhu, D. Staton, M. Popescu and D. Hawkins, "Subdomain Model for Predicting Armature Reaction Field of Surface-Mounted Permanent-Magnet Machines Accounting for Tooth-Tips," *IEEE Transactions on Magnetics*, vol. 47, no. 4, pp. 812-822, 2011.
- [29] L. J. Wu, Z. Q. Zhu, D. Staton, M. Popescu and D. Hawkins, "An Improved Sub-Domain Model for Predicting Magnetic Field of Surface-Mounted Permanent-Magnet Machines Accounting for Tooth-Tips," *IEEE Transactions on Magnetics*, vol. 47, no. 6, pp. 1693-1704, 2011.
- [30] Z. Q. Zhu, L. J. Wu and Z. P. Xia, "An Accurate Subdomain Model for Magnetic Field Computation in Slotted Surface Mounted Permanent Magnet Machines," *IEEE Transactions on Magnetics*, vol. 46, no. 4, pp. 1100-1115, 2010.
- [31] A. Ghaffari, A. Rahideh, H. Ghaffari, A. A. Vahaj and A. Mahmoudi, "Comparison between 2-D and 0-D analytical models for slotless double-sided inner armature linear permanent magnet synchronous machines," *Int Trans Electr Energ Syst*.
- [32] A. Waheed and J. Ro, "Analytical Modeling for Optimal Rotor Shape to Design Highly Efficient Line-Start Permanent Magnet Synchronous Motor," in *IEEE Access*, vol. 8, pp. 145672-145686, 2020.
- [33] Z. Q. Zhu and D. Howe, "Instantaneous Magnetic Field Distribution in Brushless Permanent Magnet DC Motors, Part III: Effect of Stator Slotting," *IEEE Transactions on Magnetics*, vol. 29, no. 1, pp. 143-151, 1993.
- [34] S. Teymoori, A. Rahideh, H. Moayed-Jahromi and M. Mardaneh, "2-D Analytical Magnetic Field Prediction for Consequent-Pole Permanent Magnet Synchronous Machines," *IEEE Transactions on Magnetics*, vol. 52, no. 6, 2016.
- [35] K. H. Shin, H. W. Cho, S. H. Lee and J. Y. Choi, "Armature Reaction Field and Inductance Calculations for a Permanent Magnet Linear Synchronous Machine Based on Subdomain Model," *IEEE Transactions on Magnetics*, vol. 53, no. 6, 2017.
- [36] S. G. Min, S. Member, B. Sarlioglu, and S. Member, "Analytical Calculation of Back - EMF Waveform for Linear The PM motors in Slotted and Slotless Structures," *IEEE Trans. Magn.*, vol. 53, no. 12, 2017.
- [37] F. Gao, Q. Wang and J. Zou, "Analytical Modeling of 3-D Magnetic Field and Performance in Magnetic Lead Screws Accounting for Magnetization Pattern," in *IEEE Transactions on Industrial Electronics*, vol. 67, no. 6, pp. 4785-4796, June 2020.
- [38] W. Tong, S. Dai, S. Li, J. Li and R. Tang, "Modeling and Analysis of Axial Flux Permanent Magnet Machines with Coexistence of Rotor Radial Deviation and Angular Eccentricity," in *IEEE Trans. on Energy Conv., Early Access*, 2020.
- [39] L. Jian, KT. Chau, Y. Gong, C. Yu and W. Li, "Analytical Calculation of Magnetic Field in Surface-Inset Permanent-Magnet Motors," *IEEE Transactions on Magnetics*, vol. 45, no. 10, pp. 4688-4691, 2009.
- [40] A. Rahideh, M. Mardaneh and T. Korakianitis, "Analytical 2D Calculations of Torque, Inductance and Back-Emf for Brushless Slotless Machines with Surface Inset Magnets," *IEEE Transactions on Magnetics*, vol. 49, no. 8, pp. 4873-4884, 2013.
- [41] T. Lubin, S. Mezani, A. Rezzoug, "Two-Dimensional Analytical Calculation of Magnetic Field and Electromagnetic Torque for Surface-Inset Permanent Magnet Motors," *IEEE Transactions on Magnetics*, vol. 48, no. 6, pp. 2080-2091, 2012.
- [42] A. Rahideh and T. Korakianitis, "Analytical Calculation of Open-Circuit Field Distribution of Slotless Brushless PM machines," *Electrical Power and Energy Systems*, vol. 44, no. 1, pp. 99-114, 2013.
- [43] O. de la Barriere, H. Ben Ahmed, M. Gabsi and M. LoBue, "Two-Dimensional Analytical Airgap Field Model of an Inset Permanent Magnet Synchronous Machine, Taking Into Account the Slotting Effect," *IEEE Transactions on Magnetics*, vol. 49, no. 4, pp. 1423-1435, 2013.
- [44] A. Parviainen, M. Niemela and J. Pyrhonen, "Modeling of Axial Flux Permanent-Magnet Machines," *IEEE Transactions on Industry Applications*, vol. 40, no. 5, pp. 1333-1340, 2004.
- [45] G. Jiao and C. D. Rahn, "Field Weakening for Radial Force Reduction in Brushless Permanent-Magnet DC Motors," *IEEE Transactions on Magnetics*, vol. 40, no. 5, pp. 3286-3292, 2004.
- [46] D. Ishak, Z. Q. Zhu and D. Howe, "Eddy-Current Loss in the Rotor Magnets of Permanent-Magnet Brushless Machines Having a Fractional Number of Slots Per Pole," *IEEE Transactions on Magnetics*, vol. 41, no. 9, pp. 2462-2469, 2005.
- [47] J. Azzouzi, G. Barakat and B. Dakyo, "Quasi-3-D Analytical Modeling of the Magnetic Field of an Axial Flux Permanent-Magnet Synchronous Machine," *IEEE Transactions on Energy Conversion*, vol. 20, no. 4, pp. 746-752, 2005.
- [48] N. Bianchi, S. Bolognani and F. Luise, "Analysis and Design of a PM Brushless Motor for High-

- Speed Operations,” *IEEE Transactions on Energy Conversion*, vol. 20, no. 3, pp. 629-637, 2005.
- [49] K. H. Shin, K. H. Jung, H. W. Cho, and J. Y. Choi, “Analytical Modeling and Experimental Verification for Electromagnetic Analysis of Tubular Linear Synchronous Machines with Axially Magnetized Permanent Magnets and Flux-Passing Iron Poles,” *IEEE Trans. Magn.*, vol. 54, no. 11, pp. 1–6, 2018.
- [50] D. Lo, H. Lawali Ali, Y. Amara, G. Barakat, and F. Chabour, “Computation of cogging force of a linear tubular flux switching permanent magnet machine using a hybrid analytical modeling,” *IEEE Trans. Magn.*, vol. 54, no. 11, 2018.
- [51] J. Bao, B. L. J. Gysen, and E. A. Lomonova, “Hybrid Analytical Modeling of Saturated Linear and Rotary Electrical Machines: Integration of Fourier Modeling,” *IEEE Trans. Magn.*, vol. 54, no. 11, 2018.
- [52] A. Rahideh and T. Korakianitis, “Analytical Magnetic Field Distribution of Slotless Brushless Machines with Inset Permanent Magnets,” *IEEE Transactions on Magnetics*, vol. 47, no. 6, pp. 1763-1774, 2011.
- [53] A. Rahideh and T. Korakianitis, “Analytical Armature Reaction Field Distribution of Slotless Brushless Machines with Inset Permanent Magnets,” *IEEE Transactions on Magnetics*, vol. 48, no. 7, pp. 2178-2191, 2012.
- [54] A. Rahideh and T. Korakianitis, “Analytical Magnetic Field Calculation of Slotted Brushless The PM machines with Surface Inset Magnets,” *IEEE Transactions on Magnetics*, vol. 48, no. 10, pp. 2633-2649, 2012.
- [55] S. Ouagued; A. Aden Diriye; Y. Amara; G. Barakat, “A General Framework Based on a Hybrid Analytical Model for the Analysis and Design of Permanent Magnet Machines,” *IEEE Transactions on Magnetics*, vol. 51, no. 11, 2015.
- [56] A. Rahideh and T. Korakianitis, “Analytical Magnetic Field Distribution of Slotless Brushless the PM motors- Part II: Open-Circuit Field and Torque Calculations,” *IET Electric Power Applications*, vol. 6, no. 9, pp. 639-651, 2012.
- [57] B. L. J. Gysen, K. J. Meessen, J. J. H. Paulides and E. A. Lomonova, “General Formulation of the Electromagnetic Field Distribution in Machines and Devices Using Fourier Analysis,” *IEEE Transactions on Magnetics*, vol. 46, no. 1, pp. 39-52, 2010.
- [58] Z. Q. Zhu and D. Howe and Z. P. Xia, “Prediction of Open-Circuit Air Gap Field Distribution in Brushless Machines Having an Inset Permanent Magnet Rotor Topology,” *IEEE Transactions on Magnetics*, vol. 30, no. 1, pp. 98-107, 1994.
- [59] Z. J. Liu, C. Bi, H. C. Tan and T. S. Low, “Modelling and Torque Analysis of Permanent Magnet Spindle Motor for Disk Drive Systems,” *IEEE Transactions on Magnetics*, vol. 30, no. 6, pp. 4317-4319, 1994.
- [60] Z. Q. Zhu, D. Howe and J. K. Mitchell, “Magnetic Field Analysis And Inductances of Brushless DC Machines with Surface-Mounted Magnets and Non-Overlapping Stator Windings,” *IEEE Transactions on Magnetics*, vol. 31, no. 3, pp. 2115-2118, 1995.
- [61] Z. J. Liu, K. J. Binns and T. S. Low, “Analysis of Eddy Current and Thermal Problems in Permanent Magnet Machines with Radial-Field Topologies,” *IEEE Transactions on Magnetics*, vol. 31, no. 3, pp. 2115-2118, 1995.
- [62] K. Ng, Z. Q. Zhu and D. Howe, “Open-Circuit Field Distribution in a Brushless Motor with Diametrically Magnetized PM Rotor, Accounting For Slotting and Eddy Current Effects,” *IEEE Transactions on Magnetics*, vol. 32, no. 5, pp. 5070-5072, 1996.
- [63] F. Deng, “Commutation-Caused Eddy-Current Losses in Permanent-Magnet Brushless DC Motors,” *IEEE Transactions on Magnetics*, vol. 33, no. 5, pp. 4310-4318, 1997.
- [64] F. Deng and T. W. Nehl, “Analytical Modeling of Eddy-Current Losses Caused by Pulse Width-Modulation Switching in Permanent-Magnet Brushless Direct-Current Motors,” *IEEE Transactions on Magnetics*, vol. 34, no. 5, pp. 3728-3736, 1998.
- [65] U. Kim and D. K. Lieu, “Magnetic Field Calculation in Permanent Magnet Motors with Rotor Eccentricity: without Slotting Effect,” *IEEE Transactions on Magnetics*, vol. 34, no. 4, pp. 2243-2252, 1998.
- [66] U. Kim and D. K. Lieu, “Magnetic Field Calculation in Permanent Magnet Motors with Rotor Eccentricity: with Slotting Effect Considered,” *IEEE Transactions on Magnetics*, vol. 34, no. 4, pp. 2253-2266, 1998.
- [67] K. Atallah, Z. Q. Zhu, D. Howe and T. S. Birch, “Armature Reaction Field and Winding Inductances of Slotless Permanent-Magnet Brushless Machines,” *IEEE Transactions on Magnetics*, vol. 34, no. 5, pp. 3737-3744, 1998.
- [68] H. Roisse, M. Hecquet and P. Brochet, “Simulations of Synchronous Machines Using an Electric-Magnetic Coupled Network Model,” *IEEE Transactions on Magnetics*, vol. 34, no. 5, pp. 3656-3659, 1998.
- [69] J. Faiz and H. Jafari, “Two-Dimensional Magnetic Field Analysis of Internal-Rotor Permanent-Magnet Motors,” *IEEE Transactions on Magnetics*, vol. 35, no. 5, pp. 4232-4237, 1999.
- [70] Y. S. Chen, Z. Q. Zhu and D. Howe, “Slotless Brushless Permanent Magnet Machines: Influence of Design Parameters,” *IEEE Transactions on Energy Conversion*, vol. 14, no. 3, pp. 686-691, 1999.
- [71] J. Wang, G. W. Jewell and D. Howe, “A General Framework for the Analysis and Design of Tubular Linear Permanent Magnet Machines,” *IEEE Transactions on Magnetics*, vol. 35, no. 3, pp. 1986-2000, 1999.
- [72] S. Vaez-Zadeh and A. H. Isfahani, “Multiobjective Design Optimization of Air-Core Linear Permanent-Magnet Synchronous Motors for Improved Thrust and Low Magnet

- Consumption” *IEEE Transactions on Magnetics*, vol. 42, no. 3, pp. 446-452, 2006.
- [73] J. H. Choi and Y. Su. Baek, “Theoretical Analysis and its Applications of a PM Synchronous Motor with Minimized Cogging Force,” *IEEE Transactions on Magnetics*, vol. 45, no. 10, pp. 4692-4695, 2009.
- [74] A. Hassanpour Isfahani, “Analytical Framework for Thrust Enhancement in Permanent-Magnet (PM) Linear Synchronous Motors with Segmented PM Poles,” *IEEE Transactions on Magnetics*, vol. 46, no. 4, pp. 1116-1122, 2010.
- [75] O. de la Barriere, S. Hlioui, H. Ben Ahmed, M. Gabsi and M. LoBue, “Three-Dimensional Analytical Modeling of a Permanent-Magnet Linear Actuator with Circular Magnets,” *IEEE Transactions on Magnetics*, vol. 46, no. 9, pp. 3608-3616, 2010.
- [76] H. Polinder and M. J. Hoeijmakers, “Eddy-Current Losses in the Segmented Surface-Mounted Magnets of a The PM machine,” *IEE Proceedings-Electric Power Applications*, vol. 146, no. 3, pp. 261-266, 1999.
- [77] J. Gan, K. T. Chau, C. C. Chan and J. Z. Jiang, “A New Surface-Inset, Permanent-Magnet, Brushless DC Motor Drive for Electric Vehicles,” *IEEE Transactions on Magnetics*, vol. 36, no. 5, pp. 3810-3818, 2000.
- [78] A. Youmssi, “A Three-Dimensional Semi-Analytical Study of the Magnetic Field Excitation in a Radial Surface Permanent-Magnet Synchronous Motor” *IEEE Transactions on Magnetics*, vol. 42, no. 12, pp. 3832-3841, 2006.
- [79] K. T. Chau, D. Zhang, J. Z. Jiang, C. Liu, and Y. Zhang, “Design of a Magnetic-Geared Outer-Rotor Permanent-Magnet Brushless Motor for Electric Vehicles,” *IEEE Transactions on Magnetics*, vol. 43, no. 6, pp. 2504-2506, 2007.
- [80] S. R. Holm, H. Polinder and J. A. Ferreira, “Analytical Modeling of a Permanent-Magnet Synchronous Machine in a Flywheel,” *IEEE Transactions on Magnetics*, vol. 43, no. 5, pp. 1955-1967, 2007.
- [81] M. Markovic and Y. Perriard, “An Analytical Determination of Eddy-Current Losses in a Configuration with a Rotating Permanent Magnet,” *IEEE Transactions on Magnetics*, vol. 43, no. 8, pp. 3380-3386, 2007.
- [82] Phil H. Mellor and R. Wrobel, “Optimization of a Multipolar Permanent-Magnet Rotor Comprising Two Arc Segments Per Pole,” *IEEE Transactions on Industry Applications*, vol. 43, no. 4, pp. 942-951, 2007.
- [83] Z. Q. Zhu, Dahaman Ishak, David Howe and Jintao Chen, “Unbalanced Magnetic Forces in Permanent-Magnet Brushless Machines with Diametrically Asymmetric Phase Windings,” *IEEE Transactions on Industry Applications*, vol. 43, no. 6, pp. 1544-1553, 2007.
- [84] R. Wrobel and P. H. Mellor, “Design Considerations of a Direct Drive Brushless Machine with Concentrated Windings,” *IEEE Transactions on Energy Conversion*, vol. 23, no. 1, pp. 1-8, 2008.
- [85] J. A. Farooq, A. Djerdir and A. Miraoui, “Analytical Modeling Approach to Detect Magnet Defects in Permanent-Magnet Brushless Motors,” *IEEE Transactions on Magnetics*, vol. 44, no. 12, pp. 4599-4604, 2008.
- [86] Bart L. J. Gysen, Koen J. Meessen, Johannes J. H. Paulides and Elena A. Lomonova, “Semi-Analytical Calculation of the Armature Reaction in Slotted Tubular Permanent Magnet Actuators,” *IEEE Transactions on Magnetics*, vol. 44, no. 11, pp. 3213-3216, 2008.
- [87] P. Virtic, P. Pisek, T. Marcic, M. Hadziselimovic and B. Stumberger, “Analytical Analysis of Magnetic Field and Back Electromotive Force Calculation of an Axial-Flux Permanent Magnet Synchronous Generator with Coreless Stator,” *IEEE Transactions on Magnetics*, vol. 44, no. 11, pp. 4333-4336, 2008.
- [88] M. Markovic and Y. Perriard, “Analytical Solution for Rotor Eddy-Current Losses in a Slotless Permanent-Magnet Motor: the Case of Current Sheet Excitation,” *IEEE Transactions on Magnetics*, vol. 44, no. 3, pp. 386-393, 2008.
- [89] M. Markovic and Y. Perriard, “Optimization Design of a Segmented Halbach Permanent-Magnet Motor Using an Analytical Model,” *IEEE Transactions on Magnetics*, vol. 45, no. 7, pp. 2955-2960, 2009.
- [90] D. Zarko, D. Ban and Thomas A. Lipo, “Analytical Solution for Electromagnetic Torque in Surface Permanent-Magnet Motors Using Conformal Mapping,” *IEEE Transactions on Magnetics*, vol. 45, no. 7, pp. 2943-2954, 2009.
- [91] B. N. Cassimere, S. D. Sudhoff and D. H. Sudhoff, “Analytical Design Model for Surface-Mounted Permanent-Magnet Synchronous Machines,” *IEEE Transactions on Energy Conversion*, vol. 24, no. 2, pp. 347-357, 2009.
- [92] P. Virtic, P. Pisek, M. Hadziselimovic, T. Marcic and B. Stumberger, “Torque Analysis of an Axial Flux Permanent Magnet Synchronous Machine by Using Analytical Magnetic Field Calculation,” *IEEE Transactions on Magnetics*, vol. 45, no. 3, pp. 1036-1039, 2009.
- [93] A. Chebak, Ph. Viarouge and Jérôme Cros, “Analytical Computation of the Full Load Magnetic Losses in the Soft Magnetic Composite Stator of High-Speed Slotless Permanent Magnet Machines,” *IEEE Transactions on Magnetics*, vol. 45, no. 3, pp. 952-955, 2009.
- [94] T. S. Kwon, S. Ki. Sul, L. Alberti and N. Bianchi, “Design and Control of an Axial-Flux Machine for a Wide Flux-Weakening Operation Region,” *IEEE Transactions on Industry Applications*, vol. 45, no. 4, pp. 1258-1266, 2009.
- [95] J. Wang, K. Atallah, R. Chin, W. M. Arshad and H. Lendenmann, “Rotor Eddy-Current Loss in Permanent-Magnet Brushless AC Machines,” *IEEE Transactions on Magnetics*, vol. 46, no. 7, pp. 2701-2707, 2010.
- [96] Y. Amara and G. Barakat, “Analytical Modeling of Magnetic Field in Surface Mounted Permanent-Magnet Tubular Linear Machines,”

- IEEE Transactions on Magnetics*, vol. 46, no. 11, pp. 3870-3884, 2010.
- [97] Z. Q. Zhu, Z. P. Xia, L. J. Wu and Geraint W. Jewell, "Analytical Modeling and Finite-Element Computation of Radial Vibration Force in Fractional-Slot Permanent-Magnet Brushless Machines," *IEEE Transactions on Industry Applications*, vol. 46, no. 5, pp. 1908-1918, 2010.
- [98] H. Bali, Y. Amara, G. Barakat, R. Ibtouen and M. Gabsi, "Analytical Modeling of Open Circuit Magnetic Field in Wound Field and Series Double Excitation Synchronous Machines," *IEEE Transactions on Magnetics*, vol. 46, no. 10, pp. 3802-3815, 2010.
- [99] P. D. Pfister and Y. Perriard, "Slotless Permanent-Magnet Machines: General Analytical Magnetic Field Calculation," *IEEE Transactions on Magnetics*, vol. 47, no. 6, pp. 739-1752, 2011.
- [100] P. Jin, Sh. Fang, H. Lin, Z. Q. Zhu, Y. Huang and X. Wang, "Analytical Magnetic Field Analysis and Prediction of Cogging Force and Torque of a Linear and Rotary Permanent Magnet Actuator," *IEEE Transactions on Magnetics*, vol. 47, no. 10, pp. 3004-3007, 2011.
- [101] A. Rahideh and T. Korakianitis, "Analytical Open-Circuit Magnetic Field Distribution of Slotless Brushless Permanent Magnet Machines with Rotor Eccentricity," *IEEE Transactions on Magnetics*, vol. 47, no. 12, pp. 4791-4808, 2011.
- [102] J. Y. Choi, S. Ho. Lee, K. Jin. Ko and S. M. Jang, "Improved Analytical Model for Electromagnetic Analysis of Axial Flux Machines with Double-Sided Permanent Magnet Rotor and Coreless Stator Windings," *IEEE Transactions on Magnetics*, vol. 47, no. 10, pp. 2760-2763, 2011.
- [103] L. Jian, G. Xu, Ch. Chris Mi, K. T. Chau and C. C. Chan, "Analytical Method for Magnetic Field Calculation in a Low-Speed Permanent-Magnet Harmonic Machine," *IEEE Transactions on Energy Conversion*, vol. 26, no. 3, pp. 862-870, 2011.
- [104] Y. Zhang, Z. Yang, M. Yu, K. Lu, Y. Ye and X. Liu, "Analysis and Design of Double-Sided Air Core Linear Servo Motor with Trapezoidal Permanent Magnets," *IEEE Transactions on Magnetics*, vol. 47, no. 10, pp. 3236-3239, 2011.
- [105] B. L. J. Gysen, K. J. Meessen, J. J. H. Paulides and E. A. Lomonova, "3-D Analytical and Numerical Modeling of Tubular Actuators with Skewed Permanent Magnets," *IEEE Transactions on Magnetics*, vol. 47, no. 9, pp. 2200-2212, 2011.
- [106] Y. Pang, Z. Q. Zhu and Z. J. Feng, "Cogging Torque in Cost-Effective Surface-Mounted Permanent-Magnet Machines," *IEEE Transactions on Magnetics*, vol. 47, no. 9, pp. 2269-2276, 2011.
- [107] A. Rahideh and T. Korakianitis, "Analytical Magnetic Field Distribution of Slotless Brushless the PM motors- Part I: Armature Reaction Field, Inductance and Rotor Eddy Current Loss Calculations," *IET Electric Power Applications*, vol. 6, no. 9, pp. 628-638, 2012.
- [108] Y. Huang, B. Ge, J. Dong, H. Lin, J. Zhu and Y. Guo, "3-D Analytical Modeling of No-Load Magnetic Field of Ironless Axial Flux Permanent Magnet Machine," *IEEE Transactions on Magnetics*, vol. 48, no. 11, pp. 2929-2932, 2012.
- [109] H. J. Shin, J. Y. Choi, H. IL. Park and S. M. Jang, "Vibration Analysis and Measurements Through Prediction of Electromagnetic Vibration Sources of Permanent Magnet Synchronous Motor Based on Analytical Magnetic Field Calculations," *IEEE Transactions on Magnetics*, vol. 48, no. 11, pp. 4216-4219, 2012.
- [110] L. J. Wu, Z. Q. Zhu, D. Staton, M. Popescu and D. Hawkins, "Analytical Model for Predicting Magnet Loss of Surface-Mounted Permanent Magnet Machines Accounting for Slotting Effect and Load," *IEEE Transactions on Magnetics*, vol. 48, no. 1, pp. 107-117, 2012.
- [111] L. J. Wu, Z. Q. Zhu, D. Staton, M. Popescu and D. Hawkins, "Analytical Model of Eddy Current Loss in Windings of Permanent-Magnet Machines Accounting for Load," *IEEE Transactions on Magnetics*, vol. 48, no. 7, pp. 2138-2151, 2012.
- [112] L. J. Wu, Z. Q. Zhu, D. Staton, M. Popescu and D. Hawkins, "Analytical Modeling and Analysis of Open-Circuit Magnet Loss in Surface-Mounted Permanent-Magnet Machines," *IEEE Transactions on Magnetics*, vol. 48, no. 3, pp. 1234-1247, 2012.
- [113] J. Fu and Ch. Zhu, "Subdomain Model for Predicting Magnetic Field in Slotted Surface Mounted Permanent-Magnet Machines with Rotor Eccentricity," *IEEE Transactions on Magnetics*, vol. 48, no. 5, pp. 1906-1917, 2012.
- [114] H. Tiegna, A. Bellara, Y. Amara and G. Barakat, "Analytical Modeling of the Open-Circuit Magnetic Field in Axial Flux Permanent-Magnet Machines with Semi-Closed Slots," *IEEE Transactions on Magnetics*, vol. 48, no. 3, pp. 1212-1226, 2012.
- [115] Y. Shen and Z. Q. Zhu, "Investigation of Permanent Magnet Brushless Machines Having Unequal-Magnet Height Pole," *IEEE Transactions on Magnetics*, vol. 48, no. 12, pp. 4815-4830, 2012.
- [116] J. M. Yon, Ph. H. Mellor, R. Wrobel, J. D. Booker and S. G. Burrow, "Analysis of Semipermeable Containment Sleeve Technology for High-Speed Permanent Magnet Machines," *IEEE Transactions on Energy Conversion*, vol. 27, no. 3, pp. 646-653, 2012.
- [117] R. P. Praveen, M. H. Ravichandran, V. T. Sadasivan Achari, V. P. Jagathy Raj, G. Madhu and G. R. Bindu, "A Novel Slotless Halbach-Array Permanent-Magnet Brushless DC Motor for Spacecraft Applications," *IEEE Transactions on Industrial Electronics*, vol. 59, no. 9, pp. 3553-3560, 2012.
- [118] M. M. Koo, S. M. Jang, Y. S. Park, H. IL. Park and J. Y. Choi, "Characteristic Analysis of Direct-Drive Wind Power Generator considering Permanent Magnet Shape and Skew Effects to Reduce Torque Ripple Based on Analytical



- Approach," *IEEE Transactions on Magnetics*, vol. 49, no. 7, pp. 3917-3920, 2013.
- [119] J. Y. Choi, H. J. Shin, S. M. Jang and S. H. Lee, "Torque Analysis and Measurements of Cylindrical Air-Gap Synchronous Permanent Magnet Couplings Based on Analytical Magnetic Field Calculations," *IEEE Transactions on Magnetics*, vol. 49, no. 7, pp. 3921-3924, 2013.
- [120] P. Jin, H. Lin, Sh. Fang, Y. Yuan, Y. Guo and Zh. Jia, "3-D Analytical Linear Force and Rotary Torque Analysis of Linear and Rotary Permanent Magnet Actuator," *IEEE Transactions on Magnetics*, vol. 49, no. 7, pp. 3989-3992, 2013.
- [121] Y. Shen and Z. Q. Zhu, "General Analytical Model for Calculating Electromagnetic Performance of Permanent Magnet Brushless Machines Having Segmented Halbach Array," *IET Electrical Systems in Transportation*, vol. 3, no. 3, pp. 57-66, 2013.
- [122] Ch. Xia, Zh. Chen, T. Shi and H. Wang, "Cogging Torque Modeling and Analyzing for Surface-Mounted Permanent Magnet Machines with Auxiliary Slots," *IEEE Transactions on Magnetics*, vol. 49, no. 9, pp. 5112-5123, 2013.
- [123] M. Rahman Mohammad, K. T. Kim and J. Hur, "Design and Analysis of a Spoke Type Motor With Segmented Pushing Permanent Magnet for Concentrating Air-Gap Flux Density," *IEEE Transactions on Magnetics*, vol. 49, no. 5, pp. 2397-2400, 2013.
- [124] L. Huang, H. Yu, M. Hu, Ch. Liu and B. Yuan, "Research on a Tubular Primary Permanent-Magnet Linear Generator for Wave Energy Conversions," *IEEE Transactions on Magnetics*, vol. 49, no. 5, pp. 1917-1920, 2013.
- [125] Y. Shen, G. Y. Liu, Z. P. Xia and Z. Q. Zhu, "Determination of Maximum Electromagnetic Torque in The The PM brushless machines Having Two-Segment Halbach Array," *IEEE Transactions on Industrial Electronics*, vol. 61, no. 2, pp. 718-729, 2014.
- [126] P. Sergeant and Alex P. M. Van den Bossche, "Influence of the Amount of Permanent-Magnet Material in Fractional-Slot Permanent-Magnet Synchronous Machines," *IEEE Transactions on Industrial Electronics*, vol. 61, no. 9, pp. 4979-4989, 2014.
- [127] Z. Chen, Ch. Xia, Q. Geng and Y. Yan, "Modeling and Analyzing of Surface-Mounted Permanent-Magnet Synchronous Machines with Optimized Magnetic Pole Shape," *IEEE Transactions on Magnetics*, vol. 50, no. 11, 2014.
- [128] F. Dubas and A. Rahideh, "Two-Dimensional Analytical Permanent-Magnet Eddy-Current Loss Calculations in Slotless PMSM Equipped With Surface-Inset Magnets," *IEEE Transactions on Magnetics*, vol. 50, no. 3, pp. 54-73, 2014.
- [129] H. Qian, H. Guo, Z. Wu and X. Ding, "Analytical Solution for Cogging Torque in Surface-Mounted Permanent-Magnet Motors with Magnet Imperfections and Rotor Eccentricity," *IEEE Transactions on Magnetics*, vol. 50, no. 8, 2014.
- [130] S. A. Hong, J. Y. Choi, S. M. Jang and K. H. Jung, "Torque Analysis and Experimental Testing of Axial Flux Permanent Magnet Couplings Using Analytical Field Calculations Based on Two Polar Coordinate Systems," *IEEE Transactions on Magnetics*, vol. 50, no. 11, 2014.
- [131] M. M. Koo, J. Y. Choi, Y. S. Park and S. M. Jang, "Influence of Rotor Overhang Variation on Generating Performance of Axial Flux Permanent Magnet Machine Based on 3-D Analytical Method," *IEEE Transactions on Magnetics*, vol. 50, no. 11, 2014.
- [132] L. J. Wu and Z. Q. Zhu, "Simplified Analytical Model and Investigation of Open-Circuit AC Winding Loss of Permanent-Magnet Machines," *IEEE Transactions on Industrial Electronics*, vol. 61, no. 9, pp. 4990-4999, 2014.
- [133] T. Wang and Zh. Zhou, "Analytical Solution of Magnetic Field Distribution in Brushless Permanent Magnet Machines with Rotor Axis Deflection," *IEEE Transactions on Magnetics*, vol. 51, no. 4, 2015.
- [134] F. Chai, P. Liang, Y. Pei and Sh. Cheng, "Analytical Method for Iron Losses Reduction in Interior Permanent Magnet Synchronous Motor," *IEEE Transactions on Magnetics*, vol. 51, no. 11, 2015.
- [135] A. Chebak, Ph. Viarouge and J. Cros, "Improved Analytical Model for Predicting the Magnetic Field Distribution in High-Speed Slotless Permanent-Magnet Machines," *IEEE Transactions on Magnetics*, vol. 51, no. 3, 2015.
- [136] A. Dalal and P. Kumar, "Analytical Model for Permanent Magnet Motor with Slotting Effect, Armature Reaction, and Ferromagnetic Material Property," *IEEE Transactions on Magnetics*, vol. 51, no. 12, 2015.
- [137] T. L. Tiang, D. Ishak, Ch. P. Lim and M. K. Mohd Jamil, "A Comprehensive Analytical Subdomain Model and Its Field Solutions for Surface-Mounted Permanent Magnet Machines," *IEEE Transactions on Magnetics*, vol. 51, no. 4, 2015.
- [138] X. Zhang, X. Liu; J. Liu and Zh. Chen, "Analytical Investigation on the Power Factor of a Flux-Modulated Permanent-Magnet Synchronous Machine," *IEEE Transactions on Magnetics*, vol. 51, no. 11, 2015.
- [139] Y. Zhou, H. Li, G. Meng, Sh. Zhou and Q. Cao, "Analytical Calculation of Magnetic Field and Cogging Torque in Surface-Mounted Permanent-Magnet Machines Accounting for Any Eccentric Rotor Shape," *IEEE Transactions on Industrial Electronics*, vol. 62, no. 6, pp. 3438-3447, 2015.
- [140] B. Dolisy, S. Mezzani, T. Lubin and J. L ev eque, "A New Analytical Torque Formula for Axial Field Permanent Magnets Coupling," *IEEE Transactions on Energy Conversion*, vol. 30, no. 3, pp. 892-899, 2015.
- [141] Zh. Qiu, J. Dai, J. Yang, X. Zhou and Y. Zhang, "Research on Rotor Eccentricity Compensation Control for Bearingless Surface-Mounted Permanent-Magnet Motors Based on an Exact Analytical Method," *IEEE Transactions on Magnetics*, vol. 51, no. 11, 2015.



- [142] H. Wang, K. Liu, B. Zhu, J. Feng, P. Ao and Zh. Zhang, "Analytical Investigation and Scaled Prototype Tests of a Novel Permanent Magnet Compulsator," *IEEE Transactions on Magnetics*, vol. 51, no. 8, 2015.
- [143] G. Heins, D. M. Ionel and M. Thiele, "Winding Factors and Magnetic Fields in Permanent-Magnet Brushless Machines With Concentrated Windings and Modular Stator Cores," *IEEE Transactions on Industry Applications*, vol. 51, no. 4, pp. 2924-2932, 2015.
- [144] A. Dalal and P. Kumar, "Analytical Model for Permanent Magnet Motor With Slotting Effect, Armature Reaction, and Ferromagnetic Material Property," *IEEE Transactions on Magnetics*, vol. 51, no. 12, 2015.
- [145] Y. Oner, Z. Q. Zhu, L. J. Wu, X. Ge, H. Zhan and J. T. Chen, "Analytical On-Load Subdomain Field Model of Permanent-Magnet Vernier Machines," *IEEE Transactions on Industrial Electronics*, vol. 63, no. 7, pp. 4105-4117, 2016.
- [146] A. J. Piña Ortega and L. Xu, "Analytical Prediction of Torque Ripple in Surface-Mounted Permanent Magnet Motors Due to Manufacturing Variations," *IEEE Transactions on Energy Conversion*, vol. 31, no. 4, pp. 1634-1644, 2016.
- [147] S. Jumayev, J. J. H. Paulides, K. O. Boynov, J. Pyrhönen and E. A. Lomonova, "3-D Analytical Model of Helical Winding The PM machines Including Rotor Eddy Currents," *IEEE Transactions on Magnetics*, vol. 52, no. 5, 2016.
- [148] Z. Zhang, Ch. Xia, H. Wang and T. Shi, "Analytical Field Calculation and Analysis of Surface Inset Permanent Magnet Machines with High Saliency Ratio," *IEEE Transactions on Magnetics*, vol. 52, no. 12, 2016.
- [149] X. Dai, Q. Liang, J. Cao, Y. Long, J. Mo and Sh. Wang, "Analytical Modeling of Axial-Flux Permanent Magnet Eddy Current Couplings with a Slotted Conductor Topology," *IEEE Transactions on Magnetics*, vol. 52, no. 2, 2016.
- [150] S. Ouagued, Y. Amara and G. Barakat, "Cogging Force Analysis of Linear Permanent Magnet Machines Using a Hybrid Analytical Model," *IEEE Transactions on Magnetics*, vol. 52, no. 7, 2016.
- [151] A. J. Piña Ortega, S. Paul, R. Islam and L. Xu, "Analytical Model for Predicting Effects of Manufacturing Variations on Cogging Torque in Surface-Mounted Permanent Magnet Motors," *IEEE Transactions on Industry Applications*, vol. 52, no. 4, pp. 3050-3061, 2016.
- [152] X. Liu, H. Hu, J. Zhao, A. Belahcen and L. Tang, "Armature Reaction Field and Inductance Calculation of Ironless BLDC Motor," *IEEE Transactions on Magnetics*, vol. 52, no. 2, 2016.
- [153] A. Dwivedi, S. K. Singh and R. K. Srivastava, "Analysis of permanent magnet brushless AC motor using Fourier transform approach," *IET Electric Power Applications*, vol. 10, no. 6, pp. 539-547, 2016.
- [154] K. Kazerooni, A. Rahideh and J. Aghaei, "Experimental Optimal Design of Slotless Brushless the PM machines Based on 2-D Analytical Model," *IEEE Transactions on Magnetics*, vol. 52, no. 5, 2016.
- [155] Y. S. Kwon and W. j. Kim, "Steady-State Modeling and Analysis of a Double-Sided Interior Permanent-Magnet Flat Linear Brushless Motor with Slot-Phase Shift and Alternate Teeth Windings," *IEEE Transactions on Magnetics*, vol. 52, no. 11, 2016.
- [156] H. Moayed-Jahromi, A. Rahideh and M. Mardaneh, "2-D Analytical Model for External Rotor Brushless The PM machines," *IEEE Transactions on Energy Conversion*, vol. 31, no. 3, pp. 1100-1109, 2016.
- [157] X. Liu, H. Hu, J. Zhao, A. Belahcen, L. Tang and L. Yang, "Analytical Solution of the Magnetic Field and EMF Calculation in Ironless BLDC Motor," *IEEE Transactions on Magnetics*, vol. 52, no. 2, 2016.
- [158] X. Yin, Y. Fang, X. Huang and P. D. Pfister, "Analytical Modeling of a Novel Vernier Pseudo-Direct-Drive Permanent-Magnet Machine," *IEEE Transactions on Magnetics*, vol. 53, no. 6, 2017.
- [159] B. Guo, Y. Huang, F. Peng, Y. Guo and J. Zhu, "Analytical Modeling of Manufacturing Imperfections in Double-Rotor Axial Flux the PM machines: Effects on Back EMF," *IEEE Transactions on Magnetics*, vol. 53, no. 6, 2017.
- [160] K. Ramakrishnan, M. Curti, D. Zarko, G. Mastinu, J. J. H. Paulides and E. A. Lomonova, "Comparative analysis of various methods for modelling surface permanent magnet machines," *IET Electric Power Applications*, vol. 11, no. 4, pp. 540-547, 2017.
- [161] L. Wu, M. Zhu, D. Wang, and Y. Fang, "A Subdomain Model for Open-Circuit Field Prediction in Dual-Stator Consequent-Pole Permanent Magnet Machines," *IEEE Trans. Magn.*, vol. 55, no. 8, pp. 1-13, 2019.
- [162] M. Hajdinjak and D. Miljavec, "Analytical Calculation of the Magnetic Field Distribution in Slotless Brushless Machines with U-Shaped Interior Permanent Magnets," *IEEE Trans. Ind. Electron.*, 2019.
- [163] M. Zhu, L. Wu, Y. Fang, and T. Lubin, "Subdomain Model for Predicting Armature Reaction Field of Dual-Stator Consequent-Pole The PM machines Accounting for Tooth-Tips," *IEEE Trans. Ind. Electron.*, vol. 3, no. 2, 2019.
- [164] W. Deng and S. Zuo, "Noise reduction of axial-flux motors by combining various pole-arc coefficients and circumferential shifting of permanent magnets: analytical approach," *IET Electr. Power Appl.*, vol. 13, no. 7, pp. 951-957, 2019.
- [165] L. Wu, S. Member, H. Yin, and D. Wang, "A Nonlinear Subdomain and Magnetic Circuit Hybrid Model for Open-Circuit Field Prediction in Surface-Mounted The PM machines," *IEEE Trans. Energy Convers.*, vol. 34, no. 3, pp. 1485-1495, 2019.
- [166] F. Ebadi, M. Mardaneh, A. Rahideh, and N. Bianchi, "Analytical Energy-Based Approaches for Cogging Torque Calculation in Surface-



- Mounted The PM motors,” no. 1, pp. 1–10.
- [167] X. Zhang, C. Zhang, J. Yu, P. Du, and L. Li, “Analytical Model of Magnetic Field of a Permanent Magnet Synchronous Motor with a Trapezoidal Halbach Permanent Magnet Array,” *IEEE Trans. Magn.*, vol. 55, no. 7, pp. 1–5, 2019.
- [168] L. J. Wu, Z. Li, D. Wang, H. Yin, X. Huang, and Z. Q. Zhu, “On-Load Field Prediction of Surface-Mounted The PM machines Considering Nonlinearity Based on Hybrid Field Model,” *IEEE Trans. Magn.*, vol. 55, no. 3, 2019.
- [169] S. T. Boroujeni, S. P. Emami, and P. Jalali, “Analytical Modeling of Eccentric PM-inset machines with a Slotless Armature,” *IEEE Trans. Energy Convers.*, vol. 34, no. 3, pp. 1466–1474, 2019.
- [170] L. Yan, Y. Liu, L. Zhang, J. Zongxia, and C. Gerada, “Magnetic Field Modeling and Analysis of Spherical Actuator with Two-dimensional Longitudinal Camber Halbach Array,” *IEEE Trans. Ind. Electron.*, vol. 66, no. 12, pp. 9112–9121, 2019.
- [171] Z. Djelloul-Khedda, K. Bouhrara, F. Dubas, A. Kechroud, and A. Tikellaline, “Analytical Prediction of Iron-Core Losses in Flux-Modulated Permanent-Magnet Synchronous Machines,” *IEEE Trans. Magn.*, vol. 55, no. 1, 2019.
- [172] S. G. Min and B. Sarlioglu, “Fast and Systematic Design Optimization of Surface-Mounted The PM machines Using Advanced Analytical Models and Subharmonic Elimination Methods,” *IEEE Trans. Magn.*, vol. 55, no. 1, pp. 1–16, 2019.
- [173] B. Guo, Y. Huang, and F. Peng, “General Analytical Modelling for Magnet Demagnetization in Surface Mounted Permanent Magnet Machines,” *IEEE Trans. Ind. Electron.*, vol. 66, no. 8, pp. 5830–5838, 2018.
- [174] S. T. Boroujeni, S. P. Emami, and P. Jalali, “Analytical Modeling of Eccentric PM-Inset Machines With a Slotless Armature,” *IEEE Trans. Energy Convers.*, vol. 34, no. 3, pp. 1466–1474, 2019.
- [175] K. H. Shin, H. W. Cho, K. H. Kim, K. Hong, and J. Y. Choi, “Analytical Investigation of the On-Load Electromagnetic Performance of Magnetic-Geared Permanent-Magnet Machines,” *IEEE Trans. Magn.*, vol. 54, no. 11, pp. 1–5, 2018.
- [176] R. Guo, H. Yu, Y. Kong, T. Xia, X. Liu, and Z. Wu, “Polar Transformed Subdomain Modeling for Double-Stator Permanent Magnet Linear Synchronous Machine,” *IEEE Trans. Magn.*, vol. 54, no. 11, pp. 1–5, 2018.
- [177] A. Rahideh, A. Ghaffari, A. Barzegar, and A. Mahmoudi, “Analytical Model of Slotless Brushless PM Linear Motors Considering Different Magnetization Patterns,” *IEEE Trans. Energy Convers.*, vol. 33, no. 4, 2018.
- [178] Y. Lu *et al.*, “Electromagnetic Force and Vibration Analysis of Permanent-Magnet-Assisted Synchronous Reluctance Machines,” *IEEE Trans. Ind. Appl.*, vol. 54, no. 5, pp. 4246–4256, 2018.
- [179] Z. Djelloul-Khedda, K. Bouhrara, F. Dubas, A. Kechroud, and B. Souleyman, “Semi-Analytical Magnetic Field Predicting in Many Structures of Permanent-Magnet Synchronous Machines Considering the Iron Permeability,” *IEEE Trans. Magn.*, vol. 54, no. 7, 2018.
- [180] L. J. Wu, Z. Li, X. Huang, Y. Zhong, Y. Fang, and Z. Q. Zhu, “A Hybrid Field Model for Open-Circuit Field Prediction in Surface-Mounted The PM machines Considering Saturation,” *IEEE Trans. Magn.*, vol. 54, no. 6, pp. 1–12, 2018.
- [181] Y. Yang, G. Liu, X. Yang, and X. Wang, “Analytical Performance Calculation of Vernier Hybrid Machine with Subdomain Method,” *Electr. Power Components Syst.*, vol. 46, no. 16–17, pp. 1883–1895, 2018.
- [182] S. G. Min and B. Sarlioglu, “Advantages and characteristic analysis of slotless rotary The PM machines in comparison with conventional laminated design using statistical technique,” *IEEE Trans. Transp. Electrification*, vol. 4, no. 2, pp. 517–524, 2018.
- [183] G. Bacco, N. Bianchi, and H. Mahmoud, “A Nonlinear Analytical Model for the Rapid Prediction of the Torque of Synchronous Reluctance Machines,” *IEEE Trans. Energy Convers.*, vol. 33, no. 3, pp. 1539–1546, 2018.
- [184] K. H. Shin, K. Hong, H. W. Cho, and J. Y. Choi, “Core Loss Calculation of Permanent Magnet Machines Using Analytical Method,” *IEEE Trans. Appl. Supercond.*, vol. 28, no. 3, pp. 1–5, 2018.
- [185] S. G. Min, G. Bramerdorfer, and B. Sarlioglu, “Analytical Modeling and Optimization for Electromagnetic Performances of Fractional-Slot The The The PM brushless machines,” *IEEE Trans. Ind. Electron.*, vol. 65, no. 5, pp. 4017–4027, 2018.
- [186] H. Hu, X. Liu, J. Zhao, and Y. Guo, “Analysis and Minimization of Detent End Force in Linear Permanent Magnet,” vol. 65, no. 3, pp. 2475–2486, 2018.
- [187] P. Liang, F. Chai, L. Chen, and Y. Wang, “Analytical prediction of no-load stator iron losses in spoke-Type permanent-magnet synchronous machines,” *IEEE Trans. Energy Convers.*, vol. 33, no. 1, pp. 252–259, 2018.
- [188] B. Hannon, P. Sergeant, and L. Dupre, “Computational-Time reduction of fourier-based analytical models,” *IEEE Trans. Energy Convers.*, vol. 33, no. 1, pp. 281–289, 2018.
- [189] M. Pourahmadi-Nakhli, A. Rahideh, and M. Mardaneh, “Analytical 2-D model of slotted brushless machines with cubic spoke-Type permanent magnets,” *IEEE Trans. Energy Convers.*, vol. 33, no. 1, pp. 373–382, 2018.
- [190] S. T. Boroujeni, P. Jalali, and N. Bianchi, “Analytical Modeling of No-Load Eccentric Slotted Surface-Mounted The PM machines: Cogging Torque and Radial Force,” *IEEE Trans. Magn.*, vol. 53, no. 12, 2017.
- [191] Z. Xue, H. Li, Y. Zhou, N. Ren, and W. Wen, “Analytical Prediction and Optimization of Cogging Torque in Surface-Mounted Permanent Magnet Machines with Modified Particle Swarm Optimization,” *IEEE Trans. Ind. Electron.*, vol. 64, no. 12, pp. 9795–9805, 2017.
- [192] L. A. J. Friedrich, J. J. H. Paulides, and E. A.

- Lomonova, "Modeling and Optimization of a Tubular Generator for Vibration Energy Harvesting Application," *IEEE Trans. Magn.*, vol. 53, no. 11, pp. 1–5, 2017.
- [193] J. De Bisschop, P. Sergeant, A. Hemeida, H. Vansompel, and L. Dupré, "Analytical Model for Combined Study of Magnet Demagnetization and Eccentricity Defects in Axial Flux Permanent Magnet Synchronous Machines," *IEEE Trans. Magn.*, vol. 53, no. 9, pp. 1–12, 2017.
- [194] Q. Wang, J. Wang, B. Zhao, Y. Li, H. Zhao, and J. Ma, "Modeling, Design Optimization, and Verifications of Permanent Magnet Linear Actuators for Structural Vibration Mitigation Applications," *IEEE Trans. Magn.*, vol. 53, no. 11, pp. 10–13, 2017.
- [195] M. Curti, S. Member, S. Member, E. A. Lomonova, and S. Member, "Magnetic Modeling of a Linear Synchronous Machine with the Spectral Element Method," *IEEE Trans. Magn.*, vol. 53, no. 11, pp. 1–6, 2017.
- [196] C. Custers, H. Jansen, and E. Lomonova, "2D semi-analytical modeling of eddy currents in multiple non-connected conducting segments," *IEEE Trans. Magn.*, vol. 53, no. 11, 2017.
- [197] N. Chiodetto, N. Bianchi, and L. Alberti, "Improved Analytical Estimation of Rotor Losses in High-Speed Surface-Mounted PM Synchronous Machines," *IEEE Trans. Ind. Appl.*, vol. 53, no. 4, pp. 3548–3556, 2017.
- [198] Z. Djelloul-Khedda, K. Boughrara, R. Ibtouen, and F. Dubas, "NonLinear analytical calculation of magnetic field and torque of switched reluctance machines," *IEEE Trans. Magn.*, vol. 53, no. 7, 2017.
- [199] T. Xia, H. Yu, Z. Chen, L. Huang, X. Liu, and M. Hu, "Design and Analysis of a Field-Modulated Tubular Linear Permanent Magnet Generator for Direct-Drive Wave Energy Conversion," *IEEE Trans. Magn.*, vol. 53, no. 6, pp. 2015–2018, 2017.
- [200] K. H. Shin, K. H. Kim, K. Hong, and J. Y. Choi, "Detent Force Minimization of Permanent Magnet Linear Synchronous Machines Using Subdomain Analytical Method Considering Auxiliary Teeth Configuration," *IEEE Trans. Magn.*, vol. 53, no. 6, 2017.
- [201] K. Guo, S. Fang, H. Lin, H. Yang, Y. Huang, and P. Jin, "3-D Analytical Analysis of Magnetic Field of Flux Reversal Linear-Rotary Permanent-Magnet Actuator," *IEEE Trans. Magn.*, vol. 53, no. 6, pp. 1–4, 2017.
- [202] P. Liang, F. Chai, Y. Li, and Y. Pei, "Analytical prediction of magnetic field distribution in spoke-type permanent-magnet synchronous machines accounting for bridge saturation and magnet shape," *IEEE Trans. Ind. Electron.*, vol. 64, no. 5, pp. 3479–3488, 2017.
- [203] S. S. Nair, J. Wang, R. Chin, L. Chen, and T. Sun, "Analytical Prediction of 3-D Magnet Eddy Current Losses in Surface Mounted The PM machines Accounting Slotting Effect," *IEEE Trans. Energy Convers.*, vol. 32, no. 2, pp. 414–423, 2017.
- [204] A. J. Piña Ortega and L. Xu, "Analytical Prediction of Torque Ripple in Surface-Mounted Permanent Magnet Motors Due to Manufacturing Variations," *IEEE Trans. Energy Convers.*, vol. 31, no. 4, pp. 1634–1644, 2016.
- [205] A. Ghaffari, A. Rahideh, A. A. Vahaj, A. Mahmoudi, and W. L. Soong, "2-D Analytical Model for Outer-Rotor Consequent-Pole Brushless The PM machines," *IEEE Trans. Energy Convers.*, 2019.
- [206] B. Guo, Y. Huang, F. Peng, J. N. Dong, and Y. Li, "Analytical Modelling of Misalignment in Axial Flux Permanent Magnet Machine," *IEEE Trans. Ind. Electron.*, 2019.
- [207] M. Hajdinjak and D. Miljavec, "Analytical Calculation of the Magnetic Field Distribution in Slotless Brushless Machines with U-Shaped Interior Permanent Magnets," *IEEE Trans. Ind. Electron.*, 2019.
- [208] W. Deng and S. Zuo, "Noise Reduction of Axial-Flux Motors by Combining Various Pole-Arc Coefficients and Circumferential Shifting of Permanent Magnets: Analytical Approach," in *IET Electric Power Applications*, vol. 13, no. 7, pp. 951–957, 7 2019.
- [209] F. Ebadi, M. Mardaneh, A. Rahideh and N. Bianchi, "Analytical Energy-Based Approaches for Cogging Torque Calculation in Surface-Mounted PM Motors," in *IEEE Transactions on Magnetics*, vol. 55, no. 5, pp. 1–10, May 2019.
- [210] X. Huang, C. Zhang, J. Chen and G. Yang, "Modeling of a Halbach Array Voice Coil Actuator via Fourier Analysis Based on Equivalent Structure," in *IEEE Transactions on Magnetics*, vol. 55, no. 8, pp. 1–6, Aug. 2019.
- [211] H. Y. Li, Z. Q. Zhu, and Y. Liu, "Optimal Flux Modulation Pole Number in Vernier Permanent Magnet Synchronous Machines," *IEEE Trans. Ind. Appl.*, 2019.
- [212] T. Carpi, Y. Lefevre, C. Henaux, J. Llibre and D. HARRIBEY, "3D Hybrid Model of the Axial Flux Motor Accounting Magnet Shape," in *IEEE Transactions on Magnetics*, 2019.
- [213] D. Golovanov and C. Gerada, "An Analytical Subdomain Model for Dual-Rotor Permanent Magnet Motor With Halbach Array," in *IEEE Transactions on Magnetics*, vol. 55, no. 12, pp. 1–16, Dec. 2019.
- [214] Q. Lu, B. Wu, Y. Yao, Y. Shen and Q. Jiang, "Analytical Model of Permanent Magnet Linear Synchronous Machines Considering End Effect and Slotting Effect," in *IEEE Transactions on Energy Conversion*, vol. 35, no. 1, pp. 139–148, March 2019.
- [215] P. Liang, F. Chai, Y. Yu and L. Chen, "Analytical Model of a Spoke-Type Permanent Magnet Synchronous In-Wheel Motor With Trapezoid Magnet Accounting for Tooth Saturation," in *IEEE Transactions on Industrial Electronics*, vol. 66, no. 2, pp. 1162–1171, Feb. 2019.
- [216] X. Zhang, C. Zhang, J. Yu, P. Du and L. Li, "Analytical Model of Magnetic Field of a Permanent Magnet Synchronous Motor With a Trapezoidal Halbach Permanent Magnet Array,"

- in *IEEE Transactions on Magnetics*, vol. 55, no. 7, pp. 1-5, July 2019.
- [217] B. Guo, Y. Huang, F. Peng and J. Dong, "General Analytical Modeling for Magnet Demagnetization in Surface Mounted Permanent Magnet Machines," in *IEEE Transactions on Industrial Electronics*, vol. 66, no. 8, pp. 5830-5838, Aug. 2019.
- [218] S. T. Boroujeni, S. P. Emami and P. Jalali, "Analytical Modeling of Eccentric PM-Inset Machines With a Slotless Armature," in *IEEE Transactions on Energy Conversion*, vol. 34, no. 3, pp. 1466-1474, Sept. 2019.
- [219] N. Elloumi, M. Bortolozzi, A. Masmoudi, M. Mezzarobba, M. Olivo and A. Tassarolo, "Numerical and Analytical Approaches to the Modeling of a Spoke Type IPM Machine With Enhanced Flux Weakening Capability," in *IEEE Transactions on Industry Applications*, vol. 55, no. 5, pp. 4702-4714, Sept.-Oct. 2019.
- [220] B. Hannon, P. Sergeant, L. Dupré and P. Pfister, "Two-Dimensional Fourier-Based Modeling of Electric Machines—An Overview," in *IEEE Transactions on Magnetics*, vol. 55, no. 10, pp. 1-17, Oct. 2019.
- [221] A. A. Vahaj, A. Rahideh and T. Lubin, "General Analytical Magnetic Model for Partitioned-Stator Flux-Reversal Machines With Four Types of Magnetization Patterns," in *IEEE Transactions on Magnetics*, vol. 55, no. 11, pp. 1-21, Nov. 2019.
- [222] L. Xu, C. Zhang, X. Zhu, M. Lin and S. Zheng, "Indirect Analytical Modeling and Analysis of V-Shaped Interior PM Synchronous Machine," in *IEEE Access*, vol. 7, pp. 173786-173795, 2019.
- [223] H. Gurleyen and E. Mese, "A Nonlinear q-Axis Inductance Modeling of a 12-Slot 10-Pole IPM Using Approximate Analytical Methods," in *IEEE Transactions on Energy Conversion*, vol. 35, no. 2, pp. 621-630, June 2019.
- [224] A. Ghaffari, A. Rahideh, H. Moayed-Jahromi, A. Vahaj, A. Mahmoudi and W. L. Soong, "2-D Analytical Model for Outer-Rotor Consequent-Pole Brushless PM Machines," in *IEEE Transactions on Energy Conversion*, vol. 34, no. 4, pp. 2226-2234, Dec. 2019.
- [225] X. Yang, B. Kou, J. Luo and H. Zhang, "A Novel Dual-consequent-pole Transverse Flux Motor and Its Analytical Modeling," in *IEEE Transactions on Industrial Electronics*. Early Access, 2020.
- [226] F. Chen, C. Zhang, J. Chen and G. Yang, "Accurate Subdomain Model for Computing Magnetic Field of Short Moving-Magnet Linear Motor With Halbach Array," in *IEEE Transactions on Magnetics*, vol. 56, no. 9, pp. 1-9, Sept. 2020.
- [227] A. Marfoli, L. Papini, P. Bolognesi and C. Gerada, "An Analytical-Numerical Approach to Model and Analyse Squirrel Cage Induction Motors," in *IEEE Trans. on En. Conv. Early Access*, 2020.
- [228] C. Tang, M. Shen, Y. Fang and P. Pfister, "Comparison of subdomain, complex permeance and relative permeance models for a wide family of permanent-magnet machines," in *IEEE Trans. on Mag. Early Access*, 2020.
- [229] V. Zamani Faradonbeh, A. Rahideh, M. Mardaneh and S. Taghipour Boroujeni, "Analytical Modeling of Flux-Reversal Permanent-Magnet Machines," in *IEEE Trans. on Energy Conv. Early Access*, 2020.
- [230] H. Zhao, C. Liu, Z. Song and W. Wang, "Analytical Modelling of a Double-Rotor Multi-Winding Machine for Hybrid Aircraft Propulsion," in *IEEE Trans. on Transp. Elec... Early Access*, 2020.
- [231] M. Forbes, W. S. P. Robertson, A. C. Zander and J. J. H. Paulidesy, "Boundary-Free Analytical Magnetic Field Calculations Including Soft Iron and Permanent Magnets Using an Iterative Discretisation Technique," in *IEEE Trans. on Mag., Early Access*, 2020.
- [232] R. Banerjee and P. Sensarma, "Improved Analytical Method to Determine Flux-linkage Characteristics of a Switched Reluctance Machine," in *IEEE Trans. on Industry App., Early Access*, 2020.
- [233] W. Tong, S. Li, X. Pan, S. Wu and R. Tang, "Analytical Model for Cogging Torque Calculation in Surface-Mounted Permanent Magnet Motors with Rotor Eccentricity and Magnet Defects," in *IEEE Trans. on Energy Conv., Early Access*, 2020.
- [234] M. Shen, P. Pfister, C. Tang and Y. Fang, "A hybrid model of permanent-magnet machines combining Fourier analytical model with finite element method, taking magnetic saturation into account," in *IEEE Trans. on Mag., Early Access*, 2020.
- [235] Y. Liu, L. Li, Q. Gao, J. Cao and Z. Sun, "An Analytical Model and Optimization of a Novel Hybrid Rotor Machine for High Torque Density," in *IEEE Trans. on Energy Conv., Early Access*, 2020.
- [236] C. Ma *et al.*, "3-D Analytical Model of Armature Reaction Field of IPMSM With Multi-Segmented Skewed Poles and Multi-Layered Flat Wire Winding Considering Current Harmonics," in *IEEE Access*, vol. 8, pp. 151116-151124, 2020.
- [237] H. Zhao, C. Liu, Z. Song, S. Liu and T. Lubin, "Analytical model for magnetic-g geared double-rotor machines and its d-q-axis determination," in *IET Electric Power Applications*, vol. 14, no. 2, pp. 175-183, 2 2020.
- [238] Y. Zhou and X. Wu, "Analytical calculation of magnetic field of bearingless flux-switching permanent-magnet machine based on doubly-salient relative permeance method," in *IET Electric Power Applications*, vol. 14, no. 5, pp. 872-884, 5 2020.
- [239] H. Shin, K. Shin, G. Jang, S. Cho, K. Jung and J. Choi, "Experimental Verification and 2D Equivalent Analysis Techniques of BLDC Motor With Permanent Magnet Overhang and Housing-Integrated Rotor Core," in *IEEE Transactions on Applied Superconductivity*, vol. 30, no. 4, pp. 1-5, June 2020.
- [240] M. M. Ghahfarokhi, E. Amiri, S. T. Boroujeni and A. D. Aliabad, "On-Load Analytical Modeling of Slotted Interior Magnet Synchronous Machines

Using Magnetic Islands Method," in *IEEE Access*, vol. 8, pp. 95360-95367, 2020.

- [241] Q. Lu, B. Wu, Y. Yao, Y. Shen and Q. Jiang, "Analytical Model of Permanent Magnet Linear Synchronous Machines Considering End Effect and Slotting Effect," in *IEEE Transactions on Energy Conversion*, vol. 35, no. 1, pp. 139-148, March 2020.
- [242] S. Wu, T. Shi, L. Guo, H. Wang and C. Xia, "Accurate Analytical Method for Magnetic Field Calculation of Interior PM Motors," in *IEEE Trans. on Energy Conv., Early Access*, 2020.
- [243] C. Ma, Y. An, H. Zhao, S. Guo, X. Yin and H. Lu, "3-D Analytical Model and Direct Measurement Method of Ultra-Thin Open-Circuit Air-Gap Field of Interior Permanent Magnet Synchronous Motor With Multi-Segmented Skew Poles and Multi-Layered Flat Wire Windings for Electric Vehicle," in *IEEE Transactions on Energy Conversion*, vol. 35, no. 3, pp. 1316-1326, Sept. 2020.
- [244] W. Ullah, F. Khan, E. Sulaiman, M. Umair, N. Ullah and B. Khan, "Analytical validation of novel consequent pole E-core stator permanent magnet flux switching machine," in *IET Electric Power Applications*, vol. 14, no. 5, pp. 789-796, 5 2020.
- [245] Y. Ni, X. Jiang, B. Xiao and Q. Wang, "Analytical Modeling and Optimization of Dual-Layer Segmented Halbach Permanent-Magnet Machines," in *IEEE Transactions on Magnetics*, vol. 56, no. 5, pp. 1-11, May 2020.
- [246] S. G. Min, "Inductance Calculation of Coreless-Type Linear PM Machines Based on Analytical Field Projection and Coil Separation Method," in *IEEE Transactions on Magnetics*, vol. 56, no. 9, pp. 1-11, Sept. 2020.
- [247] H. Lee, K. Shin, T. Bang, J. Nah and J. Choi, "Experimental Verification and Analytical Study of Influence of Rotor Eccentricity on Electromagnetic Characteristics of Permanent Magnet Machine," in *IEEE Transactions on Applied Superconductivity*, vol. 30, no. 4, pp. 1-5, June 2020.
- [248] W. Hu, X. Zhang, Y. Lei, Q. Du, L. Shi and G. Liu, "Analytical Model of Air-Gap Field in Hybrid Excitation and Interior Permanent Magnet Machine for Electric Logistics Vehicles," in *IEEE Access*, vol. 8, pp. 148237-148249, 2020.
- [249] R. Nasiri-Zarandi, A. M. Ajamloo and K. Abbaszadeh, "Design Optimization of a Transverse Flux Halbach-Array PM Generator for Direct Drive Wind Turbines," in *IEEE Transactions on Energy Conversion*, vol. 35, no. 3, pp. 1485-1493, Sept. 2020.
- [250] Z. Song, C. Liu, K. Feng, H. Zhao and J. Yu, "Field Prediction and Validation of a Slotless Segmented-Halbach Permanent Magnet Synchronous Machine for More Electric Aircraft," in *IEEE Trans. on Transp. Electrification., Early Access*, 2020.